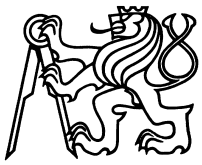

Czech Technical University in Prague
Faculty of Nuclear Sciences and Physical Engineering

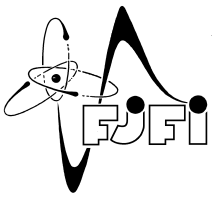

Localization on Manhattan lattices

Lokalizace na manhattanské mřížce

Master's Thesis

Author: **Bc. Tereza Štefková**

Supervisor: **prof. Ing. Igor Jex, DrSc.**

Consultant: **Ing. Martin Štefaňák, Ph.D.**

Academic year: 2017/2018

- Zadání práce -

Prohlášení

Prohlašuji, že jsem svou diplomovou práci vypracovala samostatně a použila jsem pouze podklady (literaturu, projekty, SW atd.) uvedené v přiloženém seznamu.

Nemám závažný důvod proti použití tohoto školního díla ve smyslu § 60 Zákona č. 121/2000 Sb., o právu autorském, o právech souvisejících s právem autorským a o změně některých zákonů (autorský zákon).

V Praze dne 3. 5. 2018 Tereza Štefková

Acknowledgment

I would like to express my honest gratitude to my supervisor prof. Igor Jex for suggesting this interesting topic and his useful comments. I am also very much grateful to my consultant Dr. Martin Štefaňák for his patience and kind guidance.

My thanks also belong to Dr. Aurél Gábris for the help with numerical simulations and to Dr. Adrian Ortega.

Last but not least, let me thank my family and friends for their immense support during my studies.

Název práce:

Lokalizace na manhattanské mřížce

Autor: Bc. Tereza Štefková

Obor: Matematická fyzika

Druh práce: Diplomová práce

Vedoucí práce: prof. Ing. Igor Jex, DrSc., Katedra fyziky, Fakulta jaderná a fyzikálně inženýrská, České vysoké učení technické v Praze

Konzultant: Ing. Martin Štefaňák, Ph.D., Katedra fyziky, Fakulta jaderná a fyzikálně inženýrská, České vysoké učení technické v Praze

Abstrakt: Tato práce se věnuje problematice lokalizace v kvantových procházkách na manhattanské mřížce a L-mřížce. Poté, co shrneme základní charakteristiky kvantových procházek a uvedeme problém lokalizace, ukážeme, jak lze kvantové procházky na těchto dvou orientovaných mřížkách převést na kvantové procházky na neorientované mřížce.
V případě homogenních kvantových procházek určíme obecný tvar mince, která vede k tzv. uvěznění. Pro tyto dvě orientované mřížky ukážeme, že tento efekt je triviální, neboť vede na čistě bodové spektrum evolučního operátoru. Nakonec se zabýváme Andersonovskou lokalizací na manhattanovské mřížce, u níž na základě numerických simulací docházíme k hypotéze, že Andersonovská lokalizace je přítomna pouze v případě procházek s mincemi, které jsou blízké mincím vedoucím k uvěznění.

Klíčová slova: kvantová procházka, manhattanská mřížka, L-mřížka, lokalizace

Title:

Localization on Manhattan lattices

Author: Bc. Tereza Štefková

Abstract: This thesis addresses the problem of localization in quantum walks on the Manhattan lattice and the L-lattice. Having summarized basic characteristics of quantum walks and the effect of localization in the first part, we show how the problem of quantum walks on these two oriented lattices can be formulated as quantum walks on undirected lattices.
In the case of homogeneous quantum walks we determine the general form of the so-called trapping coin. For both of these lattices it is showed that this effect is trivial since the corresponding evolution operator possesses purely point spectrum. Finally we deal with Anderson localization on the Manhattan lattice. Numerical simulations lead us to hypothesis that Anderson localization arises only in cases when the coin operators are a small perturbations of those exhibiting trapping.

Key words: quantum walk, Manhattan lattice, L-lattice, localization

Contents

Notation

$\otimes$	tensor product
diag	diagonal matrix
$\sigma(A)$	spectrum of the operator A
supp	support of a function
sup	supremum
$\mathbb{E}$	expectation value
$\langle .\vert .\rangle$	standard scalar product in $\mathbb{C}^d$
$A^\dagger$	adjoint of the operator A

Introduction

The concept of quantum walks has attracted considerable attention since their introduction by Aharanov *et al* [1] in 1993 and the seminal paper by Meyer [2]. The popularity of the research in this field can be attributed mainly to the potential utilization of quantum walks in quantum transport, quantum information theory and quantum computation.
Quantum walks can be viewed as quantum-mechanical analogues of classical random walks, which are a well-studied stochastic processes in probability theory with a wide range of applications. The term random walk was introduced by Pearson in 1905 in the context of the mathematical formulation of transport phenomena. The concept of classical random walks was used to describe for example Brownian motion as a microscopic model of diffusion [3].
The study of quantum walks has been initially motivated primarily by the development of quantum algorithms based on quantum walks that provide a considerable speed-up in comparison with their classical counterparts in terms of computational complexity. Among them the most notable is the search algorithm [4] that exhibits quadratic speed-up compared to the classical algorithms.
The interest in quantum walks has also been spurred by various experimental proposals and physical implementations of both quantum walks on a line and on a two-dimensional lattice using cold atoms in lattices, ion traps or polarization and orbital angular momentum of a photon (for a comprehensive review see [5]).
One of the motivations behind the study of quantum walks on lattices is to model transport in physical systems. The propagation of a quantum particle in homogeneous systems is known to be ballistic. In this thesis we focus mainly on the so-called effect of localization, where the ballistic propagation of the quantum particle is suppressed, typically due to the introduction of disorder to the system [6]. Physically this suppression of spreading can be interpreted as the transition from the conducting state of the material to the insulating state.

This thesis is focused on the effect of localization of discrete-time quantum walks on directed square lattices. More specifically, we address the problem of two special cases, namely the so-called Manhattan lattice [7] and L-lattice [8]. These two lattices share the property that at each node there exists two incoming and two outgoing edges. We consider both the trapping effect that arises in the case of homogeneous quantum walks and the Anderson localization which is observed in quantum walks with certain forms of static disorder.
In the case of quantum walks on the directed lattices we assume that the motion of the walker is restricted by the orientation of the underlying lattice. As a consequence, regarding the Manhattan lattice and the L-lattice, two of the four possible directions of motion are blocked at each of the vertex. This enables us to view the effective coin operators acting locally at the vertices as two-dimensional unitary matrices. In this aspect we can observe a certain resemblance between one-dimensional two-state quantum walks and quantum walks on the Manhattan lattice and the L-lattice.
Moreover, regarding the trapping effect, it is known to be trivial in the case of one-dimensional two-state

quantum walks since it appears only in certain extreme cases when the walk does not spread. Contrary to this, two-dimensional quantum walks allow for more intricate trapping effect with only a partially trapped walker at the vicinity of the origin.
On the other hand, the presence of the Anderson localization in one-dimensional two-state quantum walks has been proved for a wide range of disorder introduced via random position-dependent coin operators. For higher-dimensional quantum walks analytic results about Anderson localization are limited to certain special cases.
The above mentioned results about localization effects lead us to a question whether, despite the certain similarity with one-dimensional two-state quantum walks, quantum walks on the Manhattan lattice and the L-lattice retain the properties of two-dimensional quantum walks with respect to the trapping effect and Anderson localization.

The structure of this thesis is as follows:
First we introduce the concept of homogeneous quantum walks on the d-dimensional undirected Cartesian lattices, as we will utilize this model extensively when addressing the problem of quantum walks on the Manhattan lattice and the L-lattice. We also illustrate on this example the standard method of the time-evolution analysis of quantum walks.
In Chapter 2 we provide an introduction to the effect of localization of quantum systems with special focus on the quantum walks. We first consider the so-called trapping effect that arises in homogeneous quantum walks and is related to the spectral properties of the evolution operator for certain choices of the coin operator.
The second type of localization of our interest is the so-called Anderson localization that is typical for spatially inhomogeneous quantum systems. We briefly review the original self-adjoint model introduced by Anderson as well as the unitary Anderson model. Then we present analytic results obtained for Anderson localization of both one-dimensional and d-dimensional quantum walks in the context of the so-called dynamical localization.
To be able to employ the localization results summarized in the second chapter, we introduce a convenient method to describe quantum walks on the Manhattan lattice and the L-lattice using quantum walks on square undirected lattices. For homogeneous quantum walks on the Manhattan lattice it is shown in Chapter 3 that they can be viewed as quantum walks on undirected square lattice driven by four-dimensional coins satisfying certain restricting conditions. On the other hand, we show in Chapter 4 that homogeneous quantum walks on the L-lattice are equivalent to the so-called alternate two-dimensional quantum walks or two-dimensional split-step quantum walks which utilize only a two-dimensional coin. We also focus on the effect of trapping in the above discussed quantum walks, i. e. we determine the general form of the coin operators leading to trapping.
The last chapter is devoted to the numerical study of Anderson localization of quantum walks on the Manhattan lattice. We focus mainly on the case when the coin operator is a small perturbation of that leading to the trapping and consider only disorder introduced by random phases. We conclude the thesis with a summary of our results and outline a future prospect of further study.

Chapter 1

Quantum walks on d-dimensional Cartesian lattices

Quantum walks are quantum-mechanical counterparts of classical random walks. One of the simplest examples of discrete-time quantum walks is that of a quantum walk on a d-dimensional Cartesian lattice. In this case the quantum walker makes discrete-time steps of the same prescribed length in accordance with the underlying lattice.
The state of the walker is described by its position on the lattice and the state of its internal degree of freedom called a coin. In one time-step of a quantum walk the walker first undergoes the transformation of the coin state, which can be viewed as an analogy to the coin-flip in the case of classical random walk. Subsequently, it is shifted according to the outcome of the previous coin transformation.

1.1 Definition

Let us now introduce the concept of a quantum walk on a d-dimensional Cartesian lattice. The position of the walker on the lattice is defined by a vector from a Hilbert space spanned by

$$\mathcal{H}_p = \text{span}\{\,|\boldsymbol{x}\rangle = |x_1, \cdots, x_d\rangle \,|\, x_1, \cdots, x_d \in \mathbb{Z}\}, \tag{1.1}$$

where $x_1, \cdots, x_d$ represent the coordinates on the lattice. The walker is assigned a Hilbert space $\mathcal{H} = \mathcal{H}_c \otimes \mathcal{H}_p$, where the Hilbert space $\mathcal{H}_c$ is the so-called coin space spanned by $2d$ basis vectors, i.e.

$$\mathcal{H}_c = \text{span}\left\{\left|c_1^+\right\rangle, \left|c_1^-\right\rangle, \cdots, \left|c_d^+\right\rangle, \left|c_d^-\right\rangle\right\}, \tag{1.2}$$

with $c_j^{\pm}$ corresponding to the motion along the j-th axis in positive and negative direction, respectively. Let us assume that the walker makes steps of the same length of one unit along these axes. In order to be able to write operators acting on $\mathcal{H}$ in a compact form, we assume the steps to be represented by vectors $\{\boldsymbol{e}_j| \; j = 1, \cdots, d\}$ from the standard orthonormal basis of $\mathbb{Z}^d$.
The time evolution of a quantum walk is realized by successive application of the evolution operator

$$U = S\,(C \otimes \mathbb{I}), \tag{1.3}$$

which comprises two subsequent transformations of the state vector: the coin operator C acts solely as the transformation of the coin state and S represents the conditional shift operator which takes the form of

$$S = \sum_{x_1,\cdots,x_d \in \mathbb{Z}} \left(\sum_{j=1}^{d} \Big(\left|c_j^+\right\rangle\left\langle c_j^+\right| \otimes \left|\boldsymbol{x} + \boldsymbol{e}_j\right\rangle\langle \boldsymbol{x}| + \left|c_j^-\right\rangle\left\langle c_j^-\right| \otimes \left|\boldsymbol{x} - \boldsymbol{e}_j\right\rangle\langle \boldsymbol{x}| \Big) \right). \tag{1.4}$$

The state of the quantum walk after t steps starting with the normalized initial state localized at the origin

$$|\psi(0)\rangle = \sum_{j=1}^{d}\left(\alpha_j^+ \left|c_j^+\right\rangle + \alpha_j^- \left|c_j^-\right\rangle\right) \otimes |0, \cdots, 0\rangle\,, \qquad \sum_{j=1}^{d}(|\alpha_j^+|^2 + |\alpha_j^-|^2) = 1 \tag{1.5}$$

corresponds to

$$|\psi(t)\rangle = U^t\,|\psi(0)\rangle \tag{1.6}$$

$$= \sum_{x_1,\cdots,x_d\in\mathbb{Z}}\left(\sum_{j=1}^{d}\left(\psi_j^+(\boldsymbol{x},t)\left|c_j^+\right\rangle + \psi_j^-(\boldsymbol{x},t)\left|c_j^-\right\rangle\right) \otimes |\boldsymbol{x}\rangle\right), \tag{1.7}$$

where $\psi_j^{\pm}(\boldsymbol{x},t),\ j = 1,\ldots,d$ are components of the $2d$-component vector of the probability amplitudes $\psi(\boldsymbol{x},t)$ given as

$$\psi(\boldsymbol{x},t) = \left(\psi_1^+(\boldsymbol{x},t), \psi_1^-(\boldsymbol{x},t), \ldots, \psi_d^+(\boldsymbol{x},t), \psi_d^-(\boldsymbol{x},t)\right)^T. \tag{1.8}$$

The resulting position distribution of the quantum walk attains the following form in the above notation

$$P(\boldsymbol{x},t) = \sum_{j=1}^{d}\left(|\psi_j^+(\boldsymbol{x},t)|^2 + |\psi_j^-(\boldsymbol{x},t)|^2\right). \tag{1.9}$$

1.2 Time evolution

In the following we focus on the analysis of the time evolution of the quantum walks described above, i.e. we obtain general expressions for the probability amplitudes of the walker being at position $\boldsymbol{x}$ at time t. We only consider *spatially homogeneous* and *time-independent* quantum walks (the coin operator C does not depend on $\boldsymbol{x},\ t$) since such types of walk are the most frequented ones and can be easily solved analytically. We will refer to these simply as *homogeneous* quantum walks.

Let us now employ the method based on the Discrete-Time Fourier transform which represents the standard approach to the analysis of homogeneous quantum walk, as its dynamics attains a simple form in the momentum space. The basic principle of this method is to transform the time evolution of the probability amplitude using the Discrete-Time Fourier Transform

$$\tilde{f}(\boldsymbol{k}) = \sum_{x_1,\cdots,x_d\in\mathbb{Z}} f(\boldsymbol{x})\, e^{\mathrm{i}\boldsymbol{k}\cdot\boldsymbol{x}}, \quad k_1,\cdots,k_d \in [-\pi,\pi], \tag{1.10}$$

analyse it in the momentum domain and then transform it back to the spatial domain with the help of the Inverse Fourier Transform

$$f(\boldsymbol{x}) = \frac{1}{(2\pi)^d}\int_{-\pi}^{\pi}\cdots\int_{-\pi}^{\pi}\tilde{f}(\boldsymbol{k})\,\mathrm{e}^{-\mathrm{i}\boldsymbol{k}\cdot\boldsymbol{x}}\,\mathrm{d}k_1\ \cdots\mathrm{d}k_d. \tag{1.11}$$

In one step of the walk, only the probability amplitudes of the adjacent points can contribute to the probability amplitude $\psi(\boldsymbol{x},t)$. Consequently, the desired time evolution can be written in the form of a recurrent relation

$$\psi(\boldsymbol{x},t) = \sum_{j=1}^{d}\left(C^{2j-1}\psi(\boldsymbol{x}-\boldsymbol{e}_{2j-1},t-1) + C^{2j}\psi(\boldsymbol{x}+\boldsymbol{e}_{2j},t-1)\right), \tag{1.12}$$

with the initial condition

$$\psi(0,\cdots,0) = (\alpha_1^+, \alpha_1^-, \cdots, \alpha_d^+, \alpha_d^-)^T, \qquad \sum_{j=1}^{d}(|\alpha_j^+|^2 + |\alpha_j^-|^2) = 1, \tag{1.13}$$

where C^j corresponds to the coin operator C with zero elements except for the j-th row.
Transforming the above recurrence using the Discrete-Time Fourier Transform (1.10) we obtain the time evolution in the Fourier domain in the following form (for detailed computation see [9])

$$\tilde{\psi}(\boldsymbol{k}, t) = \tilde{U}(\boldsymbol{k})\,\tilde{\psi}(\boldsymbol{k}, t-1) = \tilde{U}^t(\boldsymbol{k})\,\tilde{\psi}(\boldsymbol{k}, 0), \tag{1.14}$$

with the transformed initial state given by $\psi(\boldsymbol{k}, 0)$ and the evolution operator in the momentum space acting as a multiplication by

$$\tilde{U}(\boldsymbol{k}) = \operatorname{diag}\left(\mathrm{e}^{\mathrm{i}k_1}, \mathrm{e}^{-\mathrm{i}k_1}, \cdots, \mathrm{e}^{\mathrm{i}k_d}, \mathrm{e}^{-\mathrm{i}k_d}\right) C. \tag{1.15}$$

As a result, the task of solving the recurrent relation (1.12) is reduced to that of finding the t-th power of $\tilde{U}(\boldsymbol{k})$ which is easily done when we diagonalize the evolution operator. The expression for the probability amplitudes in the Fourier domain then reads

$$\tilde{\psi}(\boldsymbol{k}, t) = \sum_{j=1}^{2d} \lambda_j^t(\boldsymbol{k}) \left|v_j(\boldsymbol{k})\right\rangle \left\langle v_j(\boldsymbol{k})\middle|\tilde{\psi}(\boldsymbol{k}, 0)\right\rangle, \tag{1.16}$$

where λ_j are the eigenvalues of $\tilde{U}(\boldsymbol{k})$ and v_j are the corresponding eigenvectors.
At this point we can return to the spatial domain using the Inverse Fourier Transform (1.11) thus obtaining the analytic solution of the time evolution in the Cartesian coordinates as

$$\psi(\boldsymbol{x}, t) = \frac{1}{(2\pi)^d} \sum_{j=1}^{2d} \left(\int_{-\pi}^{\pi} \cdots \int_{-\pi}^{\pi} \lambda_j^t(\boldsymbol{k}) \left|v_j(\boldsymbol{k})\right\rangle \left\langle v_j(\boldsymbol{k})\middle|\tilde{\psi}(\boldsymbol{k}, 0)\right\rangle \, \mathrm{e}^{-\mathrm{i}\boldsymbol{k}\cdot\boldsymbol{x}} \, \mathrm{d}k_1 \, \cdots \mathrm{d}k_d \right). \tag{1.17}$$

This represents the basic relation allowing us to study the effect of the initial state, the form of the shift operator and dimensionality on the dynamics of the quantum walk.

Chapter 2

Effect of localization in quantum walks

One of the interesting features of quantum walks is the so-called effect of localization, i.e. the absence of the spreading [6]. This phenomenon occurs under certain conditions imposed on the evolution operator despite the fact that the majority of homogeneous quantum walks spread ballistically.
There exist at least two types of localization in quantum walks; namely the *trapping effect* in the case of homogeneous quantum walks that stems from spectral properties of the evolution operators for special choices of the coin operator and *localization of the Anderson type* that arises in disordered systems. The latter was first studied by Anderson in [6] who argued that electrons in a crystal become trapped when exposed to external random potential on the atoms of the crystal.

2.1 The trapping effect

For the majority of homogeneous quantum walks the probability of finding the particle at the fixed position converges to zero as the number of steps t tends to infinity. This follows from the analogy with wave theory that was established in [10]. The authors showed how one-dimensional homogeneous quantum walks can be modelled as waves and derived the phase and group velocities. The maximum group velocity then determines the propagation of the peaks in the probability distribution that stems from the continuous spectrum of the evolution operator $\tilde{U}(\boldsymbol{k})$.
However, there also exist quantum walks for which the discussed probability does not vanish. This remarkable feature termed as the trapping effect is closely related to the point spectrum of the quantum walk and depends crucially on the choice of the coin operator.
In general, the eigenvalues of the unitary evolution operator (1.3) can be written as $\lambda_j(\boldsymbol{k}) = \mathrm{e}^{\mathrm{i}\omega_j(\boldsymbol{k})}$. The expression for the probability of finding the particle after t steps at the origin reads

$$P(0,\cdots,0,t) = \sum_{i=1}^{2d}\sum_{j=1}^{d}\left(|{}^{i}\psi_j^{+}(0,\cdots,0,t)|^2 + |{}^{i}\psi_j^{-}(0,\cdots,0,t)|^2\right), \tag{2.1}$$

where

$${}^{i}\psi_j^{\pm}(\boldsymbol{x},t) = \frac{1}{(2\pi)^d}\left(\int_{-\pi}^{\pi}\cdots\int_{-\pi}^{\pi}(\lambda_j^{\pm})^t(\boldsymbol{k})\left|v_j^{\pm}(\boldsymbol{k})\right\rangle\left\langle v_j^{\pm}(\boldsymbol{k})\right|\tilde{\psi}(\boldsymbol{k},0)\right\rangle\ \mathrm{e}^{-\mathrm{i}\boldsymbol{k}\cdot\boldsymbol{x}}\,\mathrm{d}k_1\ \cdots\mathrm{d}k_d\right)^{T}\cdot\boldsymbol{e}_i, \tag{2.2}$$

i.e. ${}^{i}\psi_j^{\pm}(\boldsymbol{x},t)$ is the i-th component of that part of the probability amplitude $\psi(\boldsymbol{x},t)$ corresponding to the overlap with the j-th eigenvector.
Hence we see that the expression for the probability (2.1) consists of integrals containing eigenvalues

$\lambda_j(\boldsymbol{k})$. From Riemann-Lebesgue lemma in the limit of large time t follows that only the expressions with eigenvalues λ_j independent of $\boldsymbol{k}$ contribute to the probability $P(0, \cdots, 0, +\infty)$ [11]. Hence, the existence of constant eigenvalues implies the presence of the trapping effect. At this point we remark that the trapping effect is purely a quantum phenomenon without a classical analogue since the classical random walks diffuse in case of non-zero probability of leaving the actual position.
The trapping effect has been studied extensively for quantum walks on a line and two-dimensional square lattice with a remarkable difference appearing between these two cases. It can be easily proven that the general two-dimensional as well as four-dimensional coin possesses either empty point spectrum or constant eigenvalues in the form of $\pm\lambda$ [12]. This follows from the bipartite property of the underlying lattice. As a result, trapping for two-state one-dimensional quantum walks is trivial, as the absence of the continuous spectrum leads to fully trapped walker. On the other hand, the latter allows for the trapping effect even in the case of a leaving walk (i.e. in cases when the walker is forced to leave its actual position at each step). The extent of trapping also depends on the choice of the initial state, namely on the overlap between the initial state and the eigenvectors corresponding to the constant eigenvalues. Initial states with zero overlap, i.e. orthogonal to these eigenvectors, lead to propagating walks.

A typical example of a trapping four-state quantum walk on a two-dimensional lattice is that of the Grover walk represented by the four-dimensional Grover coin

$$G = \frac{1}{2}\begin{pmatrix} -1 & 1 & 1 & 1 \\ 1 & -1 & 1 & 1 \\ 1 & 1 & -1 & 1 \\ 1 & 1 & 1 & -1 \end{pmatrix}. \tag{2.3}$$

Using the Discrete-Time Fourier transform (1.10) we obtain the transformed evolution operator $\tilde{U}(k_1, k_2)$ which, in this case, acquires the form of a four-dimensional matrix. It turns out that this matrix possesses one pair of constant eigenvalues $\lambda_{1,2} = \pm 1$ and two eigenvalues dependent on the momenta k_1, k_2 (for details see [13]). Moreover, there exists one initial state that is orthogonal to the stationary states corresponding to the constant eigenvalues, namely the state $\psi_G(k_1, k_2, 0) = \frac{1}{2}(1, -1, -1, 1)^T$. If we now consider the asymptotic probability which is given as a limit t tends to infinity in the expression (2.1), the non-zero contributions stem from the probability amplitudes ${}^i\psi_{1,2}(x, y, t)$ (2.2) corresponding to the constant eigenvalues, as mentioned above. However, the extent of the trapping, in other words the asymptotic probability of staying at the origin, also depends on the overlap of the initial state with the stationary states (see the form of (2.2)). Consequently, the special choice of the initial state $\psi_G = \frac{1}{2}(1, -1, -1, 1)^T$ orthogonal to the stationary states leads to a propagating walk, despite the non-empty point spectrum of the evolution operator.

Let us remark that trapping can also be achieved for one-dimensional quantum walk in the case of the so-called lazy walk, in which case we augment the coin space by one additional state representing no motion, i.e. the walker can move to the right, to the left or retain its current position.
Notice that in this case of three-state one-dimensional quantum walks the trapping can always be avoided by one special choice of the initial state. On the other hand, four-dimensional trapping coins can be further classified as weakly trapping if the trapping effect can be avoided for a special choice of the initial state, or strongly trapping otherwise [14].
As explained above, the presence as well as the extent of trapping also depends on the initial state, which proves not to be true for the Anderson localization. Moreover, the support of stationary states in the case of trapping is known to be finite, whereas in the case of the Anderson localization the discussed states exhibit exponential tails that are extended infinitely along the underlying lattice.

2.2 Anderson localization

While studying transport phenomena, Anderson discovered that certain forms of static disorder (evolution generated by Hamiltonian dependent on the position but constant in time) can lead to the suppression of propagation in quantum systems – presence of localized states. More specifically, the Hamiltonian of the discussed system proves to possess purely point spectrum with eigenfunctions decaying exponentially. Initially, this concept was studied in the context of self-adjoint operators on $l^2(\mathbb{Z}^d)$. For a comprehensive review we refer to [15].
However, the key object of our interest is usually the dynamics of the system given by the unitary evolution operator $U(t)$ which for Hamiltonians independent of t reads

$$U(t) = \mathrm{e}^{-\mathrm{i}Ht}. \tag{2.4}$$

For such systems it is then possible to discretize the time by a time-step of length T, introduce evolution operator $U = U(T)$ and to study the dynamics after n steps considering propagator $U(nT) = U^n$.
In the case of systems with periodic time evolution generated by $H(t+T) = H(t)$ the asymptotic behaviour is again given by $U(nT) = U(T)^n$. However, no direct relation between $U(T) = \mathrm{e}^{\mathrm{i}A}$ and the Hamiltonian of the system can be established, since we deal with time-dependent Hamiltonian [16].
Anderson localization has been studied also in the context of these periodic systems in the form of dynamical localization. This model dealing directly with the properties of the evolution operator is called the unitary Anderson model and we briefly touch upon it in this chapter, as the construction of the evolution operator is similar to that of quantum walk.

2.2.1 Anderson model for self-adjoint operators

In this section we introduce the self-adjoint Anderson model, in other words we deal with self-adjoint Hamiltonians on $l^2(\mathbb{Z}^d)$ that can be written as

$$H_\omega = H_0 + V_\omega, \tag{2.5}$$

where H_0 is the kinetic energy operator while V_ω corresponds to the random potential. We assume the random potentials V_ω to be independent, identically distributed random variables with some common distribution $\mathbb{P}_0$. This model can represent for example the motion of an electron in a crystal. The crystal itself can be viewed as a periodic lattice - $\mathbb{Z}^d$ with the electron making discrete-time steps on this lattice. In the orthonormal basis of the $l^2(\mathbb{Z}^d)$ formed by $\{\delta_j\}_{j\in\mathbb{Z}^d}$ the operator H_0 takes the following form

$$H_0(i,j) = \begin{cases} 1 & i \text{ connected to } j \\ 2d & i = j \\ 0 & \text{otherwise} \end{cases}, \tag{2.6}$$

and the potential V_ω acts as a multiplication operator.
With the help of the Discrete-Time Fourier transform it can be shown that the spectrum of H_0 is purely absolutely continuous and is equal to $\sigma(H_0) = [-2d, 2d]$, (see [15]).
As stated above, the Anderson localization is closely related to the spectral properties of the random Hamiltonian. Since we deal with a self-adjoint operator, the discussed spectrum can be written as

$$\sigma(H_\omega) = \sigma_{pp}(H_\omega) \cup \sigma_{ac}(H_\omega) \cup \sigma_{sc}(H_\omega), \tag{2.7}$$

where σ_{pp} is the purely point spectrum and σ_{ac}, σ_{sc} represent the absolutely continuous, the singular continuous spectrum, respectively.

The spectrum of the Hamiltonian has a decisive impact on the physical properties of the system. If we consider the time evolution of a state corresponding to the subspace $\mathcal{H}_{pp}$ generated by the eigenfunctions of σ_{pp}, it can be shown that such a state stays inside a compact set with high probability as time t goes to infinity. On the other hand, a state from the $\mathcal{H}_{ac}$ escapes to infinity [15].

Anderson localization has been proved for a wide range of disordered systems. Let us briefly review the main results obtained under the following assumptions on the probability distribution $\mathbb{P}_0$ of the random potentials [15]:

1. V_ω are independent, identically distributed random variables with common distribution $\mathbb{P}_0$
2. $\mathbb{P}_0$ has bounded density f
3. support of $\mathbb{P}_0$ is compact, i.e. we can assume for simplicity $\operatorname{supp}\mathbb{P}_0 = [-\lambda, \lambda]$ for some $\lambda > 0$.

One of the important properties of this model is the form of the spectrum which is known to be almost surely deterministic and equal to $\sigma(H_\omega) = [-2d, 2d] + \operatorname{supp}\mathbb{P}_0 = [-2d, 2d] + [-\lambda, \lambda]$.
Anderson localization is known to arise in one-dimensional systems for arbitrary disorder satisfying the above assumption. Moreover, in any dimension localization occurs in case of large disorder and near band edges [17].
The extent of disorder is measured by $\delta(f) = \|f\|_\infty^{-1}$ in the sense that large $\delta(f)$ implies that the support of the probability density f is extended. Localization for large disorder then means that there exists $\delta_0 > 0$ such that for $\delta(f) > \delta_0$ the resulting system exhibits localization.
Regarding localization near band edges, it is assumed that for a fixed $\lambda > 0$ there exists $\lambda_0 > 2d$ such that $2d < \lambda_0 < \lambda$. Anderson localization then arises in the interval $\sigma(H_\omega) \cap \{(\infty, -\lambda_0] \cup [\lambda_0 \cup \infty)\}$.

2.2.2 Unitary Anderson model

In the following we consider the so-called unitary Anderson model studied extensively in [16]. As mentioned above, the model deals with Hamiltonians depending periodically on time, i.e. $H(t) = H(t+T)$ for some $T > 0$.
The development of the above model has been motivated by the following physical problem. Let us assume an electron in a metal ring exposed to magnetic field that increases linearly in time, which induces a force tangent to the ring. The unitary Anderson model is concerned with the asymptotic behaviour of the electron. More specifically, it addresses the problem whether or not the imperfections of the ring prevent the energy of the electron to grow infinitely [18].
The unitary Anderson model studies unitary operators on $l^2(\mathbb{Z})$ of the form

$$U_\omega = D(\omega)U, \tag{2.8}$$

where U is a deterministic unitary operator and $D(\omega)$ introduces disorder into the system. More specifically, in the unitary Anderson model $D(\omega)$ acts as a multiplication by random phases, i.e. for every element $\psi \in l^2(\mathbb{Z})$, $k \in \mathbb{Z}$

$$D(\omega)\psi(k) = \mathrm{e}^{-\mathrm{i}\omega_k}\psi(k). \tag{2.9}$$

Similarly to the self-adjoint case, random phases are independent, identically distributed random variables taking values in $\mathbb{R}/2\pi\mathbb{Z}$ with a common distribution $\mathbb{P}$ that is absolutely continuous with a bounded density.
In analogy with the self-adjoint Anderson model, this can generate discrete evolution of a particle on one-dimensional lattice. Generally, however, the evolution operator in the case of the self-adjoint model

cannot be factorized as $e^{-itH_\omega} = e^{-itH_0}e^{-itV_\omega}$ since the operators H_0 and V_ω do not commute. Conversely, general propagator cannot be written in a form of $U_\omega = e^{-i(H_0+V\omega)}$ as discussed previously.
The deterministic part of the evolution operator for the physical system described above attains the band form of a 5 diagonal operator

$$U = \begin{pmatrix} \ddots & rt & -t^2 & & & \\ & r^2 & -rt & & & \\ & rt & r^2 & rt & -t^2 & \\ & -t^2 & -rt & r^2 & -rt & \\ & & & rt & r^2 & \\ & & & -t^2 & rt & \ddots \end{pmatrix}, \tag{2.10}$$

where r, t satisfy $r^2 + t^2 = 1$ thus ensuring the unitarity of U. As in the case of the self-adjoint Anderson model, the spectrum of the unperturbed operator U is purely absolutely continuous except for the trivial case $t = 0$ in which case the deterministic evolution operator U has purely point spectrum. On the other hand, in the other extreme case when $t = 1$ both the deterministic operator U and the perturbed evolution operator U_ω possesses purely absolutely continuous spectrum regardless of the disorder. Hence in this context the value of t provides a measure of the degree of disorder suggesting small disorder for t close to 1 and vice versa.
In [16] Anderson localization was proved for the unitary model in the context of dynamical localization. It yielded results analogous to the self-adjoint model. The authors showed that in the one-dimensional case the localization is present for any disorder.
The above described model can be generalized to arbitrary dimension using the tensor product evolution operator U_d acting in $l^2(\mathbb{Z}^d)$

$$U_d = \otimes_{j=1}^{d} U. \tag{2.11}$$

In arbitrary dimension it has been proved that localization arises in case of large disorder (i.e. for large t) or near the band edges of the spectrum.

2.3 Dynamical localization of quantum walks

Quantum walks represent a useful tool to model transport in physical systems. Due to this fact, they can be utilized to study the properties of the spreading of a quantum state including the Anderson localization. Moreover, various experimental proposals have been successfully implemented [5]. The experiments allowing for coins with random disorder can be potentially used to study Anderson localization.
Anderson localization in the case of disordered quantum walks is typically studied in the context of dynamical localization, which ensures exponential decay of the eigenfunctions as well as other significant properties of the evolution operator of the quantum walk. Let us begin this section with a summary of definitions relevant to rigorous analysis of the dynamical localization.

Definition 1. *Quantum walk driven by evolution operator U_ω exhibits*

1. ***spectral localization** [19], if U_ω has purely point spectrum, i.e.*

$$\sigma_c(U_\omega) = 0, \tag{2.12}$$

2. ***exponential localization** [19], if U_ω exhibits spectral localization and the corresponding eigenfunctions decay exponentially,*

3. ***dynamical localization*** *[20], if there exists* $C < +\infty$ *and* $\alpha > 0$ *such that for any two positions* $\boldsymbol{x}, \boldsymbol{y} \in \mathbb{Z}^d$ *and arbitrary states of the coin* c_1, c_2

$$\mathbb{E}\left(sup_{n\in\mathbb{N}} |\langle \boldsymbol{x}, c_1 | U_\omega^n | \boldsymbol{y}, c_2 \rangle|\right) \leq C \mathrm{e}^{-\alpha|\boldsymbol{x}-\boldsymbol{y}|}. \tag{2.13}$$

Theorem 1. *Dynamical localization implies exponential localization (and consequently spectral localization) [19].*

Let us now comment on the terms stated above. Spectral localization implies that there exists a complete set of square integrable eigenfunctions. We understand the exponential localization to be the analogue of the Anderson localization, as in [15]. The dynamical localization then means that the expectation value of the probability amplitude of transition between two arbitrary points stays exponentially small. Notice that when dealing with localization, spectral properties ensure neither dynamical localization, nor exponential localization.
Moreover, dynamical localization also implies that $\forall p > 0$, $|\boldsymbol{x}, c\rangle \in \mathcal{H}$ and $|X|^p$ acting as $|X|^p |\boldsymbol{x}, c\rangle = \left(\sum_{j=1}^d \max|x_j|\right)^p |\boldsymbol{x}, c\rangle$

$$\sup_{n\in\mathbb{N}} \| |X|^p U_\omega^n |\boldsymbol{x}, c\rangle \| < +\infty, \tag{2.14}$$

which means that spreading of the initial state localized at the origin is bounded [20].

2.3.1 Dynamical localization of one-dimensional quantum walks

The dynamical localization in the case of one-dimensional two-state quantum walks has been studied extensively. We will mainly focus on the disorder stemming from random phases considered by Joye *et al* in [21]. However, let us briefly remark that more general results for broader set of coin operators were derived by Werner *et al* in [22]. The authors proved that if the probability distribution at each of the vertex on the lattice possesses a positive density with respect to the Haar measure then the corresponding disordered quantum walk exhibits dynamical localization.
In [21] the authors assumed quantum walks for which the time evolution is generated by the random evolution operator U_ω of the form

$$U_\omega = S\,(C_x \otimes \mathbb{I}), \tag{2.15}$$

where S is the conditional shift operator and C_x represent the position-dependent random coin operators given as

$$C_x = \begin{pmatrix} \mathrm{e}^{-\mathrm{i}\omega_x^L} & 0 \\ 0 & \mathrm{e}^{-\mathrm{i}\omega_x^R} \end{pmatrix} \begin{pmatrix} t & -r \\ r & t \end{pmatrix}, \quad r, t \in [0,1],\ r^2 + t^2 = 1. \tag{2.16}$$

Notice that the random evolution operator can also be rewritten as a product of unperturbed operator multiplied by the random phases, i.e. $U_\omega = D(\omega)\,U$. It can be proven that this is the general form of random coin operators that are independent and identically distributed random variables in U(2), for which the probability amplitudes ψ_L and ψ_R are independent random variables while the probabilities of transition between two adjacent points are deterministic and independent of the position [21].
The evolution operator can be written in the form of (2.8) when we relabel the random phases. The deterministic part U of the random evolution operator U_ω then reads in the basis
$\{\cdots, |x-1, L\rangle, |x-1, R\rangle, |x, L\rangle\, |x, R\rangle, |x+1, L\rangle, |x+1, R\rangle \cdots\}$

$$U = \begin{pmatrix} \ddots & r & t & & & \\ & 0 & 0 & & & \\ & 0 & 0 & r & t & \\ & t & -r & 0 & 0 & \\ & & & 0 & 0 & \\ & & & t & -r & \ddots \end{pmatrix}. \tag{2.17}$$

Notice that it possesses similar band structure as in the case of the unitary Anderson model.

2.3.2 Dynamical localization of d-dimensional quantum walks

To our best knowledge, the only analytical results for dynamical localization in higher dimensions are those obtained by Joye in [20] for disorder introduced via random phases. In [20] the author considered quantum walks on the Hilbert space $\mathcal{H} = \mathbb{C}^{2d} \otimes l^2(\mathbb{Z}^d)$ driven by the random evolution operator

$$U_\omega = D(\omega)U = D(\omega)S(C \otimes \mathbb{I}), \tag{2.18}$$

where $D(\omega)$ acts as multiplication by random phases

$$D(\omega)\,|\boldsymbol{x}, c\rangle = \mathrm{e}^{\mathrm{i}\omega_{\boldsymbol{x}}^c}\,|\boldsymbol{x}, c\rangle\,, \quad \boldsymbol{x} \in \mathbb{Z}^d, \quad c \in \operatorname{span}\left\{\left|c_1^+\right\rangle, \left|c_1^-\right\rangle, \cdots, \left|c_d^+\right\rangle, \left|c_d^-\right\rangle\right\}. \tag{2.19}$$

Joye proved dynamical localization for coin operators $C \in U(2d)$ close to certain permutation matrices $C_\pi \in U(2d)$, for which the deterministic evolution operator U possesses purely point spectrum. The permutation matrices satisfying this conditions appear to be permutation operators without fixed points. Moreover, these permutations must allow for decomposition in cycles of even length and every cycle must contain both of the directions along the given axis. It can be shown that for such a coin operator the corresponding deterministic quantum walk exhibits trivial trapping effect, as the deterministic evolution operator lacks the continuous spectrum altogether.

Let us now illustrate the conditions on the permutation matrices with the help of the example of two-dimensional quantum walk on a square lattice as it will be of our interest later. Since the basis of the coin space $\mathcal{H}_c = \operatorname{span}\{c_1^+, c_1^-, c_2^+, c_2^-\}$ is four-dimensional, there exist 24 permutation coins. However, only 9 of them are permutations without fixed points. In addition, two of these are decomposed to cycles $(c_1^+, c_2^+), (c_1^-, c_2^-)$ and $(c_1^+, c_2^-), (c_1^-, c_2^+)$ that are in contradiction with the condition stated above. As a consequence, there are only 7 permutation coins that allow for purely point spectrum of the four-dimensional evolution operator.

At this point we remark, that the elements of the permutation coins can be multiplied by deterministic phases without affecting the conclusions about the trivial trapping effect and the results on the localization. Since we use the results for localization in two-dimensions extensively throughout this thesis, we will refer to these generalized permutations satisfying the above conditions as *trapping permutations*.

In order to state the results more rigorously, we include the main theorem proved by Joye in [20]

Theorem 2. *Let U_ω be defined as above and the elements of D_ω be independent, identically distributed random variables $\omega_{\boldsymbol{x}}^c$ with L^∞ density. Let $C_\pi \in U(2d)$ be a permutation matrix without fixed points satisfying the above conditions (the trapping permutation). Then there exists $\delta > 0$ such that for all U_ω with $C \in U(2d)$ satisfying $\|C - C_\pi\|_{\mathbb{C}^{2d}} \leq \delta$ the corresponding quantum walks exhibits dynamical, as well as exponential and spectral localization.*

2.4 Quantum walks with temporal disorder

So far we have only taken into consideration static disorder, for which the coin operator has been spatially inhomogeneous but constant in time. Let us now, for the sake of comparison, briefly review quantum walks with temporal disorder.
The evolution operator after t steps no longer acquires the form of U^t, it is given as

$$U(\omega, t) = U_t(\omega_t)U_{t-1}(\omega_{t-1})\cdots U_2(\omega_2)U_1(\omega_1), \tag{2.20}$$

with the evolution operator governing the j-th step reading

$$U_j(\omega_j) = S(C_j \otimes \mathbb{I}). \tag{2.21}$$

The temporal disorder is introduced via the time-dependent coin operators C_j.
In [21] authors considered disorder stemming from random phases $\omega_j^{L,R}$ that are independent, identically distributed variables with values in $\mathbb{R}/2\pi\mathbb{Z}$. The resulting random coin operators then take the form of (2.16) with the subscript referring not to the position but to the time-step. Under the additional assumption on the random phases

$$\mathbb{E}\left(\mathrm{e}^{-\mathrm{i}\omega_j^L}\right) = \mathbb{E}\left(\mathrm{e}^{-\mathrm{i}\omega_j^R}\right) = 0 \tag{2.22}$$

diffusive behaviour of the quantum walk was proved in [21].
Similar statement also holds in arbitrary dimension under certain additional assumptions on the random phases [23].

Chapter 3

Quantum walks on the Manhattan lattice

In the following two chapters we focus on quantum walks on the so-called Manhattan lattice and the so-called L-lattice. Both of these lattices are directed square lattices with two incoming and two outgoing edges at each vertex. However, in the case of the Manhattan lattice, the walker arriving at one of its vertices either continues straight on or is reflected by 90 degrees according to the orientation of the outgoing edges. On the contrary, in the case of the L-lattice the walker is forced to change direction at each step.
Motivated by the results obtained for classical random walks on the Manhattan lattice [7] and the L-lattice [8], we introduce the quantum analogue of these in the following. First of all, we show how quantum walks on these lattices can be described using 8-state quantum walk on a two-dimensional square lattice. Taking advantage of certain properties of both the Manhattan lattice and the L-lattice, we show how the description of the discussed quantum walks can be reduced to two-dimensional quantum walks on a square undirected lattice in the former case and to the so-called split-step quantum walks in the latter case, respectively.
In the following we assume that the coin-state corresponds to the direction of motion which is restricted by the orientation of the edges. The state of the whole system is described by a vector from the Hilbert space $\mathcal{H} = \mathcal{H}_c \otimes \mathcal{H}_p$ where $\mathcal{H}_c = \text{span}\{|L\rangle, |D\rangle, |U\rangle, |R\rangle\}$ is the coin space spanned by four basis states that correspond to the motion to the left, down, up and to the right. The Hilbert space
$\mathcal{H}_p = \text{span}\{|x, y\rangle \, | x, y \in \mathbb{Z}\}$ then specifies the position of the walker on the lattice.
We use the following notation

$$\psi(x, y, t) = \begin{pmatrix} \psi_L(x, y, t) \\ \psi_D(x, y, t) \\ \psi_U(x, y, t) \\ \psi_R(x, y, t) \end{pmatrix} \tag{3.1}$$

for the probability amplitudes of being at node (x, y) at time t with the given state of the coin.

3.1 Quantum walks on the Manhattan lattice

It can be easily seen that the Manhattan lattice is homogeneous with respect to cells comprised of four nodes. There exist four possible choices of these elementary cells (see Figure 3.2); however we will see that the first two of them will enable us to simplify the description of the quantum walk on the Manhattan lattice to that of two-dimensional quantum walk on a square lattice.
In the following we associate numbers 1, 2, 3 and 4 with nodes $|0, 0\rangle$, $|1, 0\rangle$, $|0, 1\rangle$ and $|1, 1\rangle$ (see Figure 3.3). Due to the direction of the edges it is necessary to use four different coins at each node which can

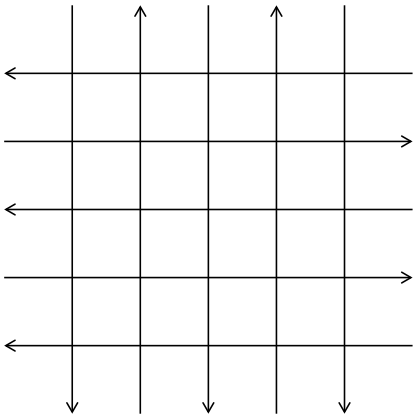

Figure 3.1: The Manhattan lattice.

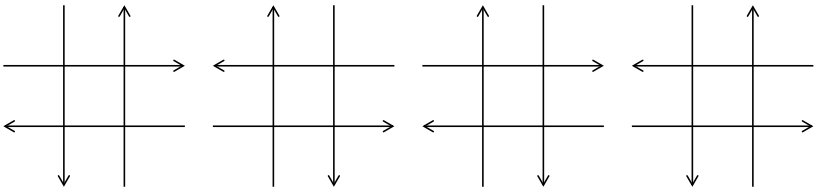

Figure 3.2: The elementary Manhattan cells.

be expressed in the basis $\{|L\rangle, |D\rangle, |U\rangle, |R\rangle\}$ as

$$C_1 = \begin{pmatrix} d_1 & b_1 & 0 & 0 \\ c_1 & a_1 & 0 & 0 \\ 0 & 0 & 1 & 0 \\ 0 & 0 & 0 & 1 \end{pmatrix}, \quad C_2 = \begin{pmatrix} a_2 & 0 & c_2 & 0 \\ 0 & 1 & 0 & 0 \\ b_2 & 0 & d_2 & 0 \\ 0 & 0 & 0 & 1 \end{pmatrix}, \quad C_3 = \begin{pmatrix} 1 & 0 & 0 & 0 \\ 0 & d_3 & 0 & b_3 \\ 0 & 0 & 1 & 0 \\ 0 & c_3 & 0 & a_3 \end{pmatrix}, \quad C_4 = \begin{pmatrix} 1 & 0 & 0 & 0 \\ 0 & 1 & 0 & 0 \\ 0 & 0 & a_4 & c_4 \\ 0 & 0 & b_4 & d_4 \end{pmatrix}, \tag{3.2}$$

where

$$\begin{pmatrix} a_j & c_j \\ b_j & d_j \end{pmatrix}, \quad j \in 1, 2, 3, 4 \tag{3.3}$$

are arbitrary two-dimensional unitary coins that effectively act at the vertices.
As mentioned above, the Manhattan lattice can be composed of the elementary cells shown in Figure 3.3. Let us now identify each of the cells with a point on the two-dimensional square lattice (for the coordinates on this lattice we use letters n, m). The correspondence between the coordinates on the lattices is given as

$$(n, m) \longleftrightarrow \begin{array}{l} 1\colon (x, y) = (2n, 2m) \\ 2\colon (x, y) = (2n+1, 2m) \\ 3\colon (x, y) = (2n, 2m+1) \\ 4\colon (x, y) = (2n+1, 2m+1) \end{array}, \tag{3.4}$$

where the numbers 1,2,3,4 label the position inside the cell (Figure 3.3).
The state of the walker on the Manhattan lattice can be described by the position of the corresponding

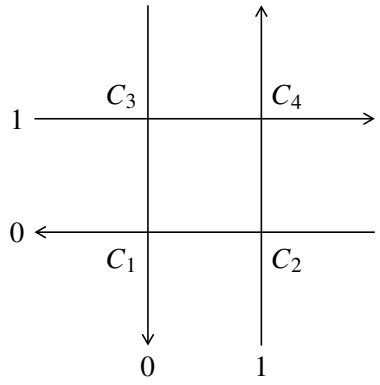

Figure 3.3: The elementary Manhattan cell.

cell on the square lattice (labelled by n, m), position of the node inside the cell (labelled by 1,2,3 or 4) and the coin state. In terms of (3.1) it means,

$$\psi(n,m,t) = \begin{pmatrix} \psi_1(n,m,t) \\ \psi_2(n,m,t) \\ \psi_3(n,m,t) \\ \psi_4(n,m,t) \end{pmatrix}, \text{ where } \quad \psi_i(n,m,t) = \begin{pmatrix} \psi_L(x,y,t) \\ \psi_D(x,y,t) \\ \psi_U(x,y,t) \\ \psi_R(x,y,t) \end{pmatrix}. \tag{3.5}$$

The probability amplitude of the walker being at the position n, m at time t is then given by a 16-component vectors $\psi(n,m,t)$.

Let us assume that four different coins $C_1,\ C_2,\ C_3$ and C_4 (3.2) act at each of the four nodes inside each of the cells. When describing one step of the quantum walk in a cell, we consider four possibilities:

- the walker comes from the outside of the cell and continues to another cell,
- the walker comes from the inside of the given cell and moves to another cell,
- the walker moves inside of the given cell,
- the walker comes from the outside and continues inside of the cell.

Labelling the state by i or o according to if the walker comes from the inside or the outside of the given cell enables us to reduce the dimension of the coin operator acting in the cell to 8. This follows from the fact that the combination of i, o and the coin state is unique within each of the cells.
The 8-dimensional coin operator in the basis $\{|L\rangle_o, |D\rangle_o, |U\rangle_o, |R\rangle_o, |L\rangle_i, |D\rangle_i, |U\rangle_i, |R\rangle_i\}$ reads

$$C_M = \begin{pmatrix} 0 & 0 & 0 & 0 & d_1 & b_1 & 0 & 0 \\ 0 & 0 & 0 & 0 & c_1 & a_1 & 0 & 0 \\ 0 & 0 & 0 & 0 & 0 & 0 & a_4 & c_4 \\ 0 & 0 & 0 & 0 & 0 & 0 & b_4 & d_4 \\ a_2 & 0 & c_2 & 0 & 0 & 0 & 0 & 0 \\ 0 & d_3 & 0 & b_3 & 0 & 0 & 0 & 0 \\ b_2 & 0 & d_2 & 0 & 0 & 0 & 0 & 0 \\ 0 & c_3 & 0 & a_3 & 0 & 0 & 0 & 0 \end{pmatrix}. \tag{3.6}$$

However, as we will see, a convenient choice of the cell enables us to simplify the above description to two-dimensional quantum walks driven by four-dimensional coin satisfying certain restricting condition. Focusing closely on one step of the two-dimensional quantum walk on the corresponding square lattice we see that it consists of two subsequent steps inside the cells. Namely the state of the walker entering the cell is a linear combination of states $(\alpha\,|L\rangle+\beta\,|U\rangle)\otimes|1,0\rangle$ and $(\gamma\,|R\rangle+\delta\,|D\rangle)\otimes|0,1\rangle$ (see Figure 3.3). Firstly, this state is transformed at vertices $(1,0)$ and $(0,1)$ by the coins C_2 and C_3, respectively. Subsequently, it is shifted inside the cell according to the directions of the edges, undergoes the transformation by the coins C_1 and C_4, and leaves the cell. This transformation of the initial state entering the cell can be written as

$$\begin{aligned}
|L\rangle &\mapsto a_2d_1\,|L\rangle + a_2c_1\,|D\rangle + a_4b_2\,|U\rangle + b_2b_4\,|R\rangle\\
|D\rangle &\mapsto b_1d_3\,|L\rangle + a_1d_3\,|D\rangle + c_3c_4\,|U\rangle + c_3d_4\,|R\rangle\\
|U\rangle &\mapsto c_2d_1\,|L\rangle + c_1c_2\,|D\rangle + a_4d_2\,|U\rangle + b_4d_2\,|R\rangle\\
|R\rangle &\mapsto b_1b_3\,|L\rangle + a_1b_3\,|D\rangle + a_3c_4\,|U\rangle + a_3d_4\,|R\rangle\,.
\end{aligned} \tag{3.7}$$

The corresponding coin operating on the square lattice then attains the following form

$$C_M = \begin{pmatrix} a_2\,d_1 & b_1\,d_3 & c_2\,d_1 & b_1\,b_3\\ a_2\,c_1 & a_1\,d_3 & c_1\,c_2 & a_1\,b_3\\ a_4\,b_2 & c_3\,c_4 & a_4\,d_2 & a_3\,c_4\\ b_2\,b_4 & c_3\,d_4 & b_4\,d_2 & a_3\,d_4 \end{pmatrix} = \begin{pmatrix} d_1 & b_1 & 0 & 0\\ c_1 & a_1 & 0 & 0\\ 0 & 0 & a_4 & c_4\\ 0 & 0 & b_4 & d_4 \end{pmatrix}\begin{pmatrix} a_2 & 0 & c_2 & 0\\ 0 & d_3 & 0 & b_3\\ b_2 & 0 & d_2 & 0\\ 0 & c_3 & 0 & a_3 \end{pmatrix}, \tag{3.8}$$

and its unitarity is equivalent to the unitarity of matrices (3.3) which represent unitary transformations at the nodes of the Manhattan lattice.
We see that a quantum walk on the Manhattan lattice can be represented by a quantum walk on two-dimensional square lattice driven by coin in the form of(3.8) with the conditional step operator given by

$$\begin{aligned}
S = \sum_{n,m\in\mathbb{Z}} \Big(&|L\rangle\langle L|\otimes|n-1,m\rangle\langle n,m| + |D\rangle\langle D|\otimes|n,m-1\rangle\langle n,m| +\\
&|U\rangle\langle U|\otimes|n,m+1\rangle\langle n,m| + |R\rangle\langle R|\otimes|n+1,m\rangle\langle n,m| \Big).
\end{aligned} \tag{3.9}$$

With the help of the Discrete-Time Fourier Transform (1.10) we obtain the evolution operator in the Fourier domain as

$$\tilde{U}_M(k,l) = \begin{pmatrix} \mathrm{e}^{-\mathrm{i}k} & 0 & 0 & 0\\ 0 & \mathrm{e}^{-\mathrm{i}l} & 0 & 0\\ 0 & 0 & \mathrm{e}^{\mathrm{i}l} & 0\\ 0 & 0 & 0 & \mathrm{e}^{\mathrm{i}k} \end{pmatrix} C_M. \tag{3.10}$$

In the following we utilize the correspondence between the quantum walk on the Manhattan lattice and the two-dimensional quantum walk on the square lattice to derive some of the interesting properties of the Manhattan walks.

3.2 Trapping effect in quantum walks on the Manhattan lattice

Let us now analyse under which conditions the quantum walks described above exhibit the trapping effect by imposing conditions on the spectrum of the matrix $\tilde{U}_M(k,l)$. More specifically, our aim is to determine the form of the general trapping coin C_M (3.8). We consider the most general case when the

quantum walk has 4 different coins at each node in a cell.

We proceed as follows: we impose restrictions on the characteristic equation for the transformed evolution operator $\tilde{U}_M(k,l)$ and solve it with respect to the parameters of the coin operator (3.8). The characteristic equation reads

$$\det\left(\tilde{U}_M(k,l) - \lambda\mathbb{I}\right) = 0. \tag{3.11}$$

The presence of the trapping effect is related to the existence of a constant eigenvalue. Moreover, in the case of four-state two-dimensional quantum walks the discussed constant eigenvalues always come in pairs. The determinant of the transformed evolution operator $\tilde{U}(k,l)$ can be written as a product

$$\det\tilde{U}_M(k,l) = \det\left(\mathrm{diag}\left(\mathrm{e}^{-\mathrm{i}k}, \mathrm{e}^{-\mathrm{i}l}, \mathrm{e}^{\mathrm{i}l}, \mathrm{e}^{\mathrm{i}k}\right)\right)\det C_M = \det C_M. \tag{3.12}$$

In other words, the determinant of $\tilde{U}_M(k,l)$ is independent of k,l. On the other hand, determinant of a matrix is also equal to the product of its eigenvalues. As a result, we can write down the characteristic equation in the form of

$$\det\left(\tilde{U}_M(k,l) - \lambda\mathbb{I}\right) = \left(\mathrm{e}^{\mathrm{i}\varphi} - \lambda\right)\left(-\mathrm{e}^{\mathrm{i}\varphi} - \lambda\right)\left(\mathrm{e}^{\mathrm{i}\omega(k,l)} - \lambda\right)\left(\mathrm{e}^{-\mathrm{i}\omega(k,l)} - \lambda\right) = 0, \tag{3.13}$$

where $\pm\mathrm{e}^{\mathrm{i}\varphi}$ represent the pair of constant eigenvalues.
Let us now determine, under which conditions $\mathrm{e}^{\mathrm{i}\varphi}$ is an eigenvalue of the transformed evolution operator $\tilde{U}_M(k,l)$. That is, we solve the equation

$$\det\left(\tilde{U}_M(k,l) - \mathrm{e}^{\mathrm{i}\varphi}\mathbb{I}\right) = 0, \tag{3.14}$$

with respect to the parameters of the two-dimensional coin operators (3.3). The solution (for details we refer to the Appendix A) of this equation is given as

$$C_i = \begin{pmatrix} 0 & c_i \\ b_i & 0 \end{pmatrix}, \quad C_j = \begin{pmatrix} 0 & c_j \\ b_j & 0 \end{pmatrix}, \quad C_k = \begin{pmatrix} 0 & c_k \\ b_k & 0 \end{pmatrix}, \quad C_l = \begin{pmatrix} a_l & c_l \\ b_l & d_l \end{pmatrix}, \tag{3.15}$$

where i, j, k, l are pair-wise distinct indexes from $\{1,2,3,4\}$ with the additional condition reading

$$\mathrm{e}^{4\mathrm{i}\varphi} - b_i b_j b_k b_l \mathrm{e}^{2\mathrm{i}\varphi} - c_i c_j c_k c_l \mathrm{e}^{2\mathrm{i}\varphi} - b_i b_j b_k c_i c_j c_k (a_l d_l - b_l c_l) = 0. \tag{3.16}$$

Let us now assume without a loss of generality, that the index l in (3.15) is equal to 4. The characteristic equation for the solution given by (3.15) attains a simple form

$$\lambda^4 - (b_1 b_2 b_3 b_4 + c_1 c_2 c_3 c_4)\lambda^2 - b_1 b_2 b_3 c_1 c_2 c_3 (a_4 d_4 - b_4 c_4) = 0, \tag{3.17}$$

that does not depend on k,l. As a consequence, the trapping effect in case of quantum walks driven by the coin (3.8) is trivial since the evolution operator $\tilde{U}_M(k,l)$ possess only the point spectrum.

At this point we restrict ourselves to solutions of (3.16) in the form of SU(2). An arbitrary SU(2) matrix can be parametrized as

$$M = \begin{pmatrix} a\,\mathrm{e}^{\mathrm{i}\alpha} & b\,\mathrm{e}^{\mathrm{i}\beta} \\ -b\,\mathrm{e}^{-\mathrm{i}\beta} & a\,\mathrm{e}^{-\mathrm{i}\alpha} \end{pmatrix}, \quad a^2 + b^2 = 1, \quad a, b, \alpha, \beta \in \mathbb{R}. \tag{3.18}$$

Using this parametrization for matrices (3.15) we obtain the general SU(2) solution of (3.16) dependent on 6 real parameters as

$$C_i = \begin{pmatrix} 0 & \mathrm{e}^{\mathrm{i}\alpha_i} \\ -\mathrm{e}^{-\mathrm{i}\alpha_i} & 0 \end{pmatrix},\ i \in \{1,2,3\}, \quad C_{4\pm} = \begin{pmatrix} \pm\sqrt{1 - \frac{\cos^2(4\varphi)}{\cos^2(\alpha_1+\alpha_2+\alpha_3+\beta)}}\,\mathrm{e}^{\mathrm{i}\alpha} & \frac{\cos(4\varphi)}{\cos(\alpha_1+\alpha_2+\alpha_3+\beta)} e^{\mathrm{i}\beta} \\ -\frac{\cos(4\varphi)}{\cos(\alpha_1+\alpha_2+\alpha_3+\beta)} e^{-\mathrm{i}\beta} & \pm\sqrt{1 - \frac{\cos^2(4\varphi)}{\cos^2(\alpha_1+\alpha_2+\alpha_3+\beta)}}\,\mathrm{e}^{-\mathrm{i}\alpha} \end{pmatrix}. \tag{3.19}$$

Note that since the choice of the parameter φ is arbitrary, matrices $C_{4_\pm}$ cover all SU(2) coin operators. The characteristic equation for this solution reads

$$\lambda^4 - 2\cos(4\varphi)\lambda^2 + 1 = 0, \tag{3.20}$$

with the solution acquiring the form

$$\lambda_{1,2} = \pm e^{i\varphi}. \tag{3.21}$$

We conclude that the trapping effect in the case of a homogeneous quantum walk on the Manhattan lattice is trivial since the trapping coins possess only the point spectrum. The absence of the continuous part of the spectrum causes the suppression of the propagation of the resulting quantum walk.

Chapter 4

Quantum walks on the L-lattice

Let us now turn to the quantum walks on the L-lattice, in which case we follow similar approach as in the case of the Manhattan lattice and find that their description can be reduced to a certain type of two-dimensional quantum walks utilizing only two-dimensional coin operators.
Analogously to the Manhattan lattice the L-lattice (see Figure 4.1) is homogeneous with respect to cells (see Figure 4.3). As a consequence, the description of the homogeneous quantum walk on this lattice can be reduced to that of the 8-state quantum walk on a square lattice driven by the coin operator

$$C_L = \begin{pmatrix} 0 & 0 & c_1 & 0 & 0 & a_1 & 0 & 0 \\ a_2 & 0 & 0 & 0 & 0 & 0 & 0 & c_2 \\ 0 & 0 & 0 & d_3 & b_3 & 0 & 0 & 0 \\ 0 & b_4 & 0 & 0 & 0 & 0 & d_4 & 0 \\ 0 & a_4 & 0 & 0 & 0 & 0 & c_4 & 0 \\ 0 & 0 & 0 & c_3 & a_3 & 0 & 0 & 0 \\ b_2 & 0 & 0 & 0 & 0 & 0 & 0 & d_2 \\ 0 & 0 & d_1 & 0 & 0 & b_1 & 0 & 0 \end{pmatrix}. \tag{4.1}$$

However, the description can be further simplified to two-dimensional coins when we take into consideration four subsequent steps as follows.
The L-lattice can be composed of two types of vertices shown in Figure 4.2. Although there are four different directions of motion, the quantum walk on the L-lattice can be defined using only two coin states. This follows from the fact that when we consider four subsequent steps starting for example from the vertex with the coin operator C_1 which acts on the coin states $|L\rangle$ and $|R\rangle$ we necessarily arrive at vertex C_1 with coin states $|L\rangle$ and $|R\rangle$. In other words, the evolution operator comprised of even number of steps always mixes only two of the four possible coin states, namely the states $|L\rangle$ and $|R\rangle$ or the states $|D\rangle$ and $|U\rangle$. Hence we introduce the following identification of the coin states $|L\rangle, |D\rangle = |1\rangle$ and $|R\rangle, |U\rangle = |2\rangle$, where

$$\{|1\rangle, |2\rangle\} = \left\{ \begin{pmatrix} 1 \\ 0 \end{pmatrix}, \begin{pmatrix} 0 \\ 1 \end{pmatrix} \right\}. \tag{4.2}$$

This allows us to introduce the evolution operator in the following form (considering quantum walk starting from the first vertex with the coin operator C_1, see Figure 4.3)

$$U_L = S_{DU}\, C_4\, S_{LR}\, C_3\, S_{DU}\, C_2\, S_{LR}\, C_1, \tag{4.3}$$

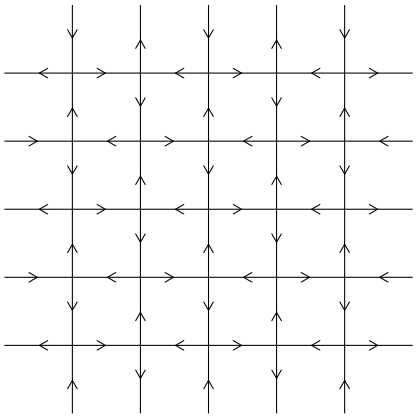

Figure 4.1: The L-lattice.

Figure 4.2: The elementary L-lattice vertices

where the shift operators S_{LR} and S_{UD} correspond to the motion along the x axis and y axis, respectively. Explicitly,

$$S_{LR} = \sum_{x,y\in\mathbb{Z}} \Big(|1\rangle\langle 1| \otimes |x-1,y\rangle\langle x,y| + |2\rangle\langle 2| \otimes |x+1,y\rangle\langle x,y| \Big) \tag{4.4}$$

$$S_{DU} = \sum_{x,y\in\mathbb{Z}} \Big(|1\rangle\langle 1| \otimes |x,y-1\rangle\langle x,y| + |2\rangle\langle 2| \otimes |x,y+1\rangle\langle x,y| \Big), \tag{4.5}$$

and the two-dimensional unitary coin operators acting on the two types of vertices are given as

$$C_j = \begin{pmatrix} a_j & c_j \\ b_j & d_j \end{pmatrix}, \quad j \in \{1,2,3,4\}. \tag{4.6}$$

The Discrete-Time Fourier transform then yields the time evolution in the momentum space as

$$\tilde{\psi}(k,l,t+1) = \tilde{U}_L(k,l)\,\tilde{\psi}(k,l,t) = \begin{pmatrix} \mathrm{e}^{-\mathrm{i}l} & 0 \\ 0 & \mathrm{e}^{\mathrm{i}l} \end{pmatrix} C_4 \begin{pmatrix} \mathrm{e}^{-\mathrm{i}k} & 0 \\ 0 & \mathrm{e}^{\mathrm{i}k} \end{pmatrix} C_3 \begin{pmatrix} \mathrm{e}^{-\mathrm{i}l} & 0 \\ 0 & \mathrm{e}^{\mathrm{i}l} \end{pmatrix} C_2 \begin{pmatrix} \mathrm{e}^{-\mathrm{i}k} & 0 \\ 0 & \mathrm{e}^{\mathrm{i}k} \end{pmatrix} C_1 \tilde{\psi}(k,l,t). \tag{4.7}$$

We see that quantum walks on the L-lattice can be viewed as quantum walks on an undirected square lattice utilizing only two-dimensional coin operators with the shift operator modified as described above.

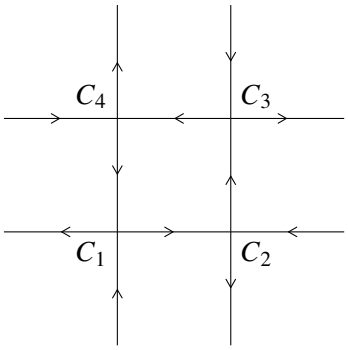

Figure 4.3: The elementary L-lattice cell.

4.1 Relation to the two-dimensional alternate and the two-dimensional split-step quantum walks

Quantum walks driven by the evolution operator in a form similar to (4.3) have been studied previously in the context of the so-called two-dimensional alternate quantum walks introduced in [24]. The authors considered the evolution generated by

$$U_{\text{alternate}} = S_{DU}\, H\, S_{LR}\, H, \tag{4.8}$$

where H is the well-know Hadamard coin

$$H = \frac{1}{\sqrt{2}} \begin{pmatrix} 1 & 1 \\ 1 & -1 \end{pmatrix}. \tag{4.9}$$

They argued that the probability distribution of this alternate quantum walk starting with the initial state $\psi(0,0) = \frac{1}{\sqrt{2}}(1,\mathrm{i})^T$ is identical to the probability distribution of the two-dimensional walk with the Grover coin (2.3) for the specific choice of the unique non-trapping initial state $\psi_G(0,0,0) = \frac{1}{2}(1,-1,-1,1)^T$. Let us also remark that quantum walks on the L-lattice with rotation coins are equivalent to the so-called two-dimensional split-step quantum walks studied in [25]. In this case the evolution is governed by

$$U_{\text{split}} = S_{DU}\, R(\theta_2)\, S_{LR}\, R(\theta_1), \tag{4.10}$$

with the rotation coins

$$R(\theta_j) = \begin{pmatrix} \cos\theta_j & -\sin\theta_j \\ \sin\theta_j & \cos\theta_j \end{pmatrix}, \quad j = 1,2, \quad \theta_j \in [-\frac{\pi}{2}, \frac{\pi}{2}]. \tag{4.11}$$

We will comment on the split-step quantum walks and the results obtained in [25] later in the context of localization in quantum walks on the L-lattice.

4.2 Trapping effect in quantum walks on the L-lattice

Similarly to the analysis of the trapping effect on the Manhattan lattice, let us now turn to the analysis of the general trapping coins in quantum walks on the L-lattice. This can be again formulated as a problem

of determining the form of the coin operators $C_1,\ C_2,\ C_3,\ C_4$ satisfying the characteristic equation for the transformed evolution operator $\tilde{U}_L(k,l)$ with the constant eigenvalue $\mathrm{e}^{\mathrm{i}\varphi},\ \varphi \in \mathbb{R}$ which reads

$$\det\left(\tilde{U}_L(k,l) - \mathrm{e}^{\mathrm{i}\varphi}\mathbb{I}\right) = 0. \tag{4.12}$$

Since this characteristic equation holds for arbitrary $k, l \in [-\pi, \pi]$, it can be readily separated. After some algebra (for details we refer to the Appendix A), we obtain the general form of the trapping coins as (A.10) or (A.11). The characteristic equation for this solution is independent of k, l which leads to purely point spectrum.

In the case of the general trapping coins in quantum walks on the L-lattice, we obtained only the point spectrum. As a result, we conclude that the trapping effect is trivial, similarly to that of the quantum walks on the Manhattan lattice.

For the L-lattice this conclusion could have been anticipated from the form of the evolution operator that in the momentum space acquires the form of a two-dimensional matrix as in the case of two-state one-dimensional quantum walk.

Chapter 5

Localization in quantum walks on the Manhattan lattice

In the previous two chapters we dealt with homogeneous quantum walks on the Manhattan lattice and the L-lattice. Let us now focus on spatially inhomogeneous quantum walks on the Manhattan lattice.
Motivated by results obtained by Joye [20] we consider static disorder introduced by random phases. That is, the evolution operator of the corresponding inhomogeneous quantum walks attains the following form

$$U_\omega = D(\omega)S(C \otimes \mathbb{I}), \tag{5.1}$$

where $D(\omega)$ is a diagonal matrix acting as a multiplication by random phases in the form $\mathrm{e}^{\mathrm{i}\omega(x,y,c)}$, $c \in \{L, D, U, R\}$. Joye proved localization for quantum walks on square lattices for coins close to the trapping permutation matrices. This property is measured by the matrix norm

$$\|A\|_{\mathbb{C}^4} = \sqrt{\lambda_{max}(A^\dagger A)}, \quad A \in \mathbb{C}^{4,4}, \tag{5.2}$$

where $\lambda_{\max}(A)$ denotes the largest eigenvalue of the matrix A.
Let us now employ numerical simulations to estimate the asymptotic behaviour of the disordered quantum walks on the Manhattan lattice. We infer this from two characteristics: the probability distribution and the time evolution of its variance σ^2. Since we deal with two-dimensional lattice, we analyse the cross-section of the probability distribution averaged over the number of iterations.
We depict the resulting cross-section of the probability distribution in a logarithmic plot. As a consequence, we anticipate the localized quantum walks to exhibit peak consisting of two linear functions meeting at the origin, since in this case exponential decay of the probability distribution is expected. The cross-section of the probability distribution behaving as a quadratic function suggests diffusive spreading. This is characteristic for classical random walks for which the probability distribution after t steps is proportional to

$$P(x,t) \sim \mathrm{e}^{\frac{-x^2}{2\sigma^2}}, \quad \sigma^2 = 2Dt. \tag{5.3}$$

The second feature of our interest is the long-time behaviour of the variance

$$\sigma^2(t) = \sum_{x,y\in\mathbb{Z}} \left((x-\mu(x))^2 + (y-\mu(y))^2\right) P(x,y,t), \tag{5.4}$$

where $\mu(x), \mu(y)$ are the mean values of the variables x, y. Since the variance measures the expected deviation of the random variables from its mean, it provides a good estimate of the spreading of the probability distribution. The propagation of the unperturbed quantum walk is known to be ballistic, i.e.

$\sigma^2 \sim t^2$. On the other hand, the spreading of the classical random walks behaves as $\sigma^2 \sim t$. Finally, since the probability distribution of the localized quantum walk decays exponentially, we expect the corresponding variance to saturate, i.e. $\sigma^2 \sim 1$.

5.1 Elementary Manhattan cell with four identical coins

Let us first consider the case utilizing the same coin at each of the 4 nodes of the elementary Manhattan cell, i.e. $C_j = C$ for $j = 1, 2, 3, 4$. Consequently, the coin operator (3.8) attains the following form

$$C_M = \begin{pmatrix} ad & bd & cd & b^2 \\ ac & ad & c^2 & ab \\ ab & c^2 & ad & ac \\ b^2 & cd & bd & ad \end{pmatrix}. \tag{5.5}$$

Let us first restrict ourselves to $C \in \mathrm{SU}(2)$. Using the parametrization for general $M \in \mathrm{SU}(2)$

$$M = \begin{pmatrix} \sqrt{1-\rho^2}\mathrm{e}^{\mathrm{i}\alpha} & \rho\,\mathrm{e}^{\mathrm{i}\beta} \\ -\rho\,\mathrm{e}^{-\mathrm{i}\beta} & \sqrt{1-\rho^2}\mathrm{e}^{-\mathrm{i}\alpha} \end{pmatrix}, \quad \rho, \alpha, \beta \in \mathbb{R}, \quad \rho \in [0, 1] \tag{5.6}$$

we obtain the coin operator in the form

$$C_M = \begin{pmatrix} (1-\rho^2) & -\rho\sqrt{1-\rho^2}\,\mathrm{e}^{\mathrm{i}(-\beta-\alpha)} & \rho\sqrt{1-\rho^2}\,\mathrm{e}^{\mathrm{i}(\beta-\alpha)} & \rho^2\,\mathrm{e}^{-2\mathrm{i}\beta} \\ \rho\sqrt{1-\rho^2}\,\mathrm{e}^{\mathrm{i}(\alpha+\beta)} & (1-\rho^2) & \rho^2\,\mathrm{e}^{2\mathrm{i}\beta} & -\rho\sqrt{1-\rho^2}\,\mathrm{e}^{\mathrm{i}(\alpha-\beta)} \\ -\rho\sqrt{1-\rho^2}\,\mathrm{e}^{\mathrm{i}(\alpha-\beta)} & \rho^2\,\mathrm{e}^{2\mathrm{i}\beta} & (1-\rho^2) & \rho\sqrt{1-\rho^2}\,\mathrm{e}^{\mathrm{i}(\alpha+\beta)} \\ \rho^2\,\mathrm{e}^{-2\mathrm{i}\beta} & \rho\sqrt{1-\rho^2}\,\mathrm{e}^{\mathrm{i}(\beta-\alpha)} & -\rho\sqrt{1-\rho^2}\,\mathrm{e}^{\mathrm{i}(-\beta-\alpha)} & (1-\rho^2) \end{pmatrix}. \tag{5.7}$$

According to the results obtained by Joye, we expect localization for ρ close to 1, as in this case the coin operator satisfies the condition of being close to one of the trapping permutation matrices.
Figure 5.1 depicts the dependence of the norm of $\|C_M - C_\pi\|$ on the value of ρ. In the case of 4 identical coins C_π is the anti-diagonal permutation matrix. We see that the norm as a function of ρ increases as we decrease ρ, which means that we should expect the presence of localization only for ρ very close to 1.

5.1.1 Numerical simulations

In the case of the coin operator C_M (5.5), we can take advantage of the symmetries of the resulting quantum walk and consider cross-sections only along the x axis without a loss of generality. Moreover, we assume the distribution to be centred around the origin and set $\mu(x) = \mu(y) = 0$ when computing the variance.
In our simulations we examined the dependence of the probability distribution and the time evolution of the variance on the value of the parameter ρ. We performed 10000 iterations for quantum walks with 100 steps for different values of ρ restricting ourselves to real SU(2) matrices, i.e. we set $\alpha, \beta = 0$. We assumed the random phases to be independent and identically distributed random numbers in $[0, 2\pi]$.
Results obtained from numerical simulations suggest that in the case of four identical coins in the elementary Manhattan cell we observe 3 types of asymptotic behaviour with respect to the value of ρ. For ρ close to 1 the corresponding quantum walk exhibits localization which is characterised by linear decay of the averaged probability distribution in the semilogarithmic plot (see the left plot in Figure 5.2). Moreover, we see that the spreading given by the variance of this averaged distribution saturates as the time t increases (see the right plot in Figure 5.2).

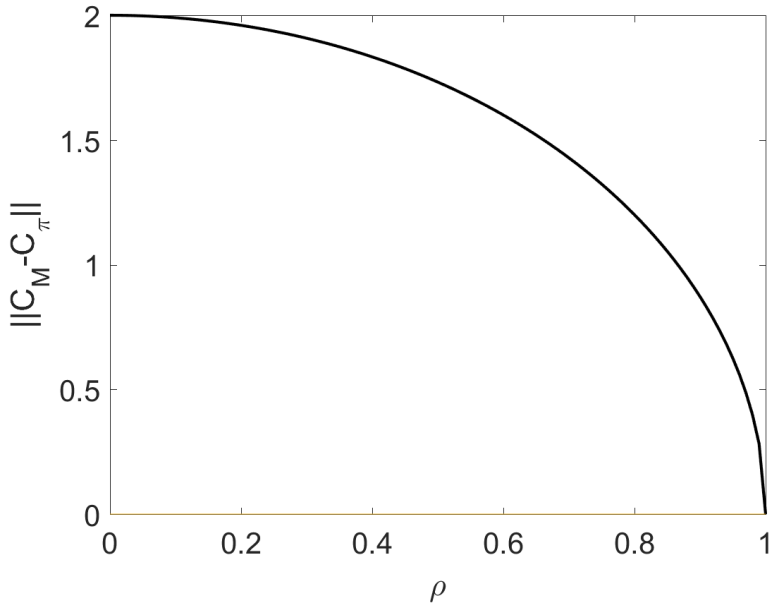

Figure 5.1: Dependence of the norm $\|C_M - C_\pi\|$ on the value of the parameter ρ

Decreasing the parameter ρ, the width of the peak in the probability distribution as well as the rate of spreading grows. For $\rho \in [0.3, 0.8]$ the averaged probability distribution decays quadratically (the left plot in Figure 5.4) and the variance increases linearly in time (the right plot in Figure 5.4). These features are attributed to diffusive propagation of the resulting quantum walk.
In the case of small ρ it can be seen that ballistic propagation starts to prevail. This we deduce from the shape of the averaged probability distribution that exhibits two peaks propagating proportionately to the number of steps t (see the left plot in Figure 5.5). Moreover, the variance grows quadratically (see the right plot in Figure 5.5) as expected in the case of ballistic spreading.
However, the analysis is inconclusive for $\rho \in [0.80, 0.98]$ (Figure 5.3). Therefore, we performed 10 iterations with the number of steps increased to 400. We remark that the demands on the computational time in the case of 400 steps and 10 iterations are comparable to the previous regime when we performed 10000 iterations for 100 steps of the quantum walk.
The results obtained for this increased number of steps suggest that the transition between localized regime and diffusion occurs in the interval $\rho \in [0.80, 0.90]$. This can be inferred from Figure 5.6 and 5.7 where it is shown that while spreading saturates for $\rho \sim 0.90$, propagation of the quantum walk with $\rho \sim 0.80$ is nearly diffusive.
However, we cannot exclude the possibility of localization setting in after more then 400 steps. Nevertheless, the number of steps in our simulations is limited by rapidly increasing time needed to perform one iteration, as well as memory demands. That is, since we deal with a square lattice, the time complexity as well as the space complexity grows quadratically with the size of the underlying lattice. Without parallelization the time needed to perform 10000 iterations for quantum walk with 100 steps reached approximately 120 hours.

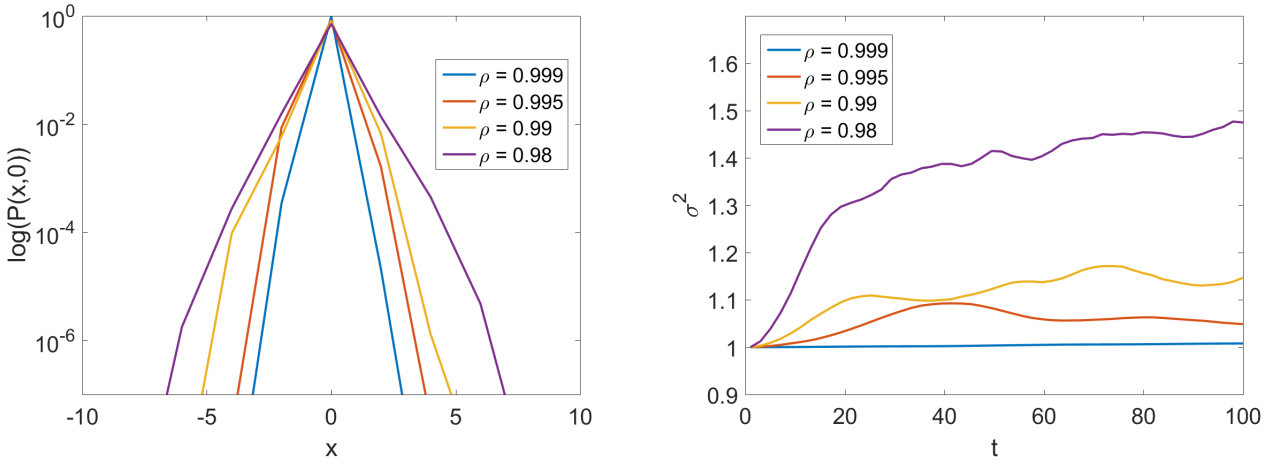

Figure 5.2: Cross-section of the probability distribution after 100 steps averaged over 10000 iterations, semilogplot (on the left). The time-dependence of the corresponding variance σ^2 (on the right). The parameter of the coin operator set to $\rho = 0.999$, $\rho = 0.995$, $\rho = 0.99$ and $\rho = 0.98$.

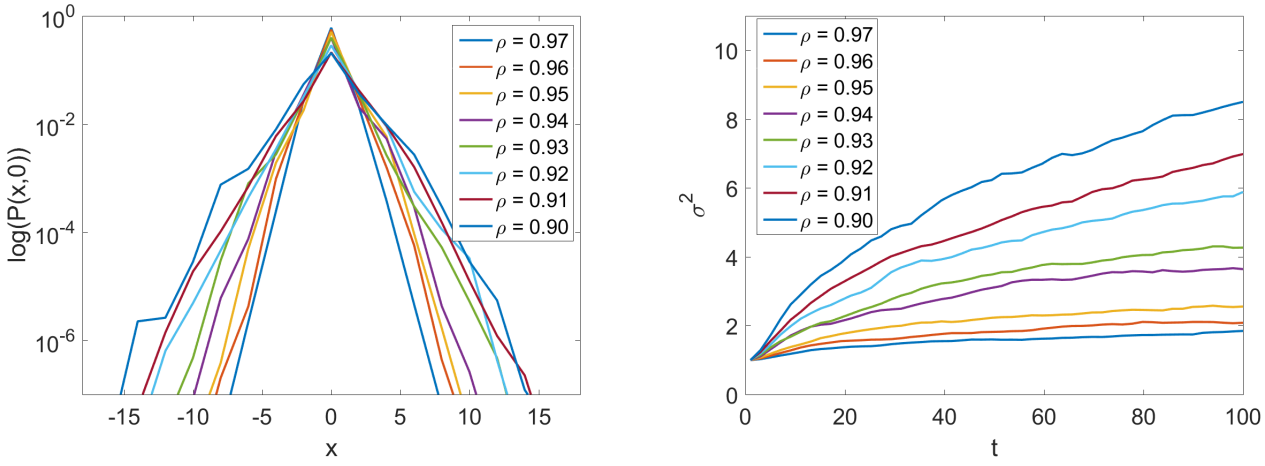

Figure 5.3: Cross-section of the probability distribution after 100 steps averaged over 10000 iterations, semilogplot (on the left). The time-dependence of the corresponding variance σ^2 (on the right). The parameter of the coin operator set to $\rho = 0.97$, $\rho = 0.96$, $\rho = 0.95$, $\rho = 0.94$, $\rho = 0.93$, $\rho = 0.92$, $\rho = 0.91$ and $\rho = 0.90$.

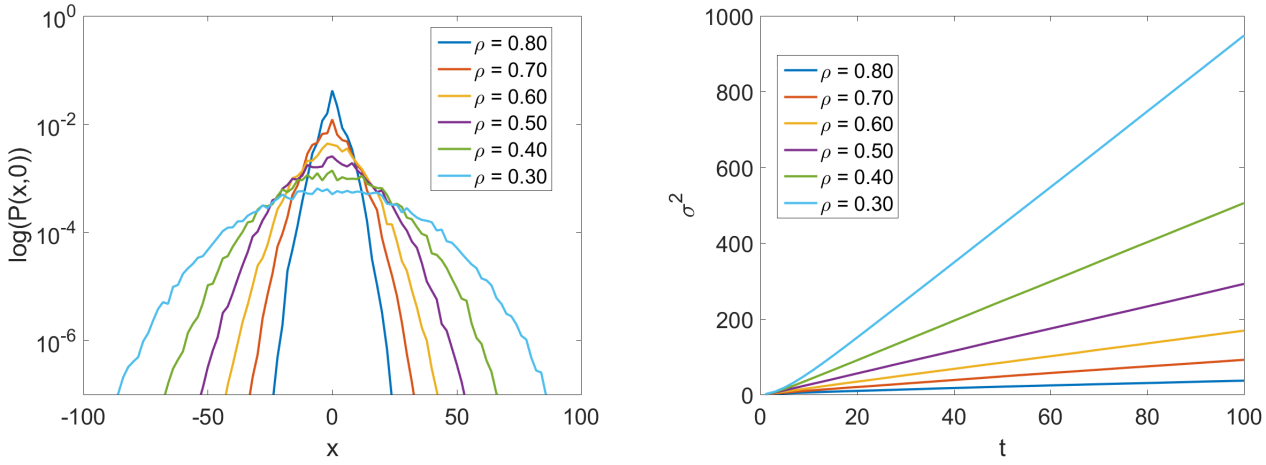

Figure 5.4: Cross-section of the probability distribution after 100 steps averaged over 10000 iterations, semilogplot (on the left). The time-dependence of the corresponding variance σ^2 (on the right). The parameter of the coin operator set to $\rho = 0.80$, $\rho = 0.70$, $\rho = 0.60$, $\rho = 0.50$, $\rho = 0.40$ and $\rho = 0.30$.

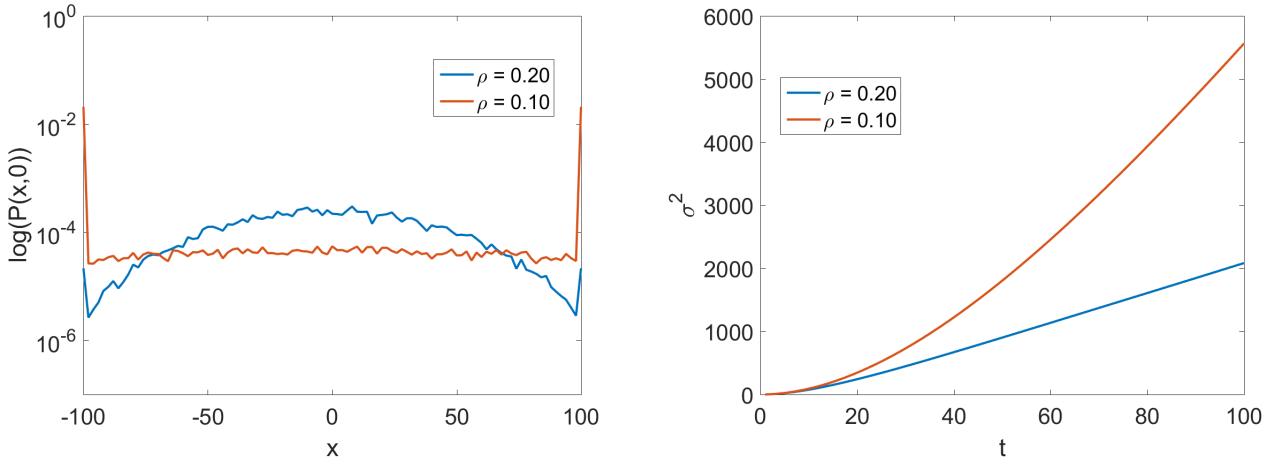

Figure 5.5: Cross-section of the probability distribution after 100 steps averaged over 10000 iterations, semilogplot (on the left). The time-dependence of the corresponding variance σ^2 (on the right). The parameter of the coin operator set to $\rho = 0.20$ and $\rho = 0.10$.

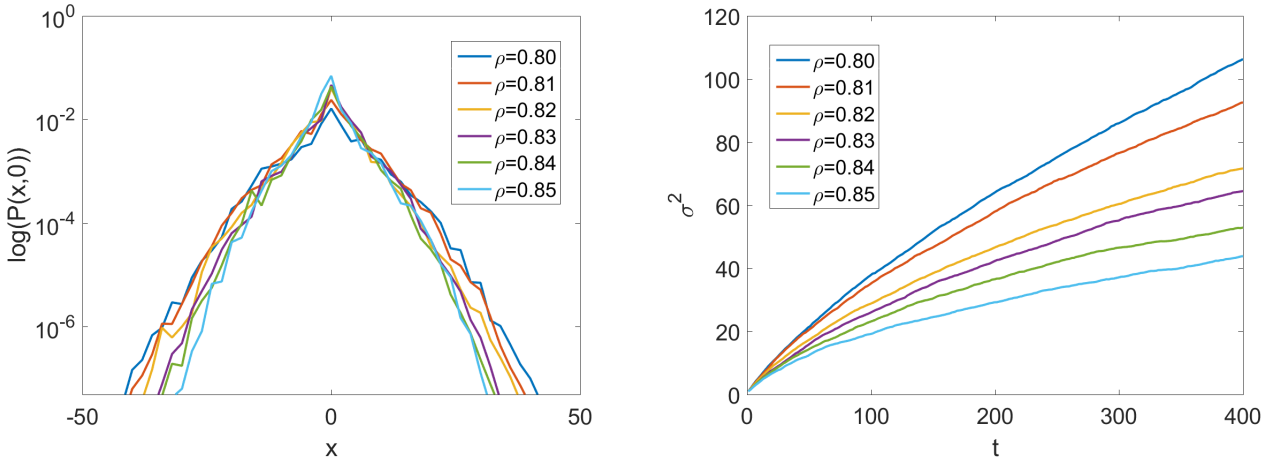

Figure 5.6: Cross-section of the probability distribution after 400 steps averaged over 10 iterations, semilogplot (on the left). The time-dependence of the corresponding variance σ^2 (on the right). The parameter of the coin operator set to $\rho = 0.80$, $\rho = 0.81$, $\rho = 0.82$, $\rho = 0.83$, $\rho = 0.84$ and $\rho = 0.85$.

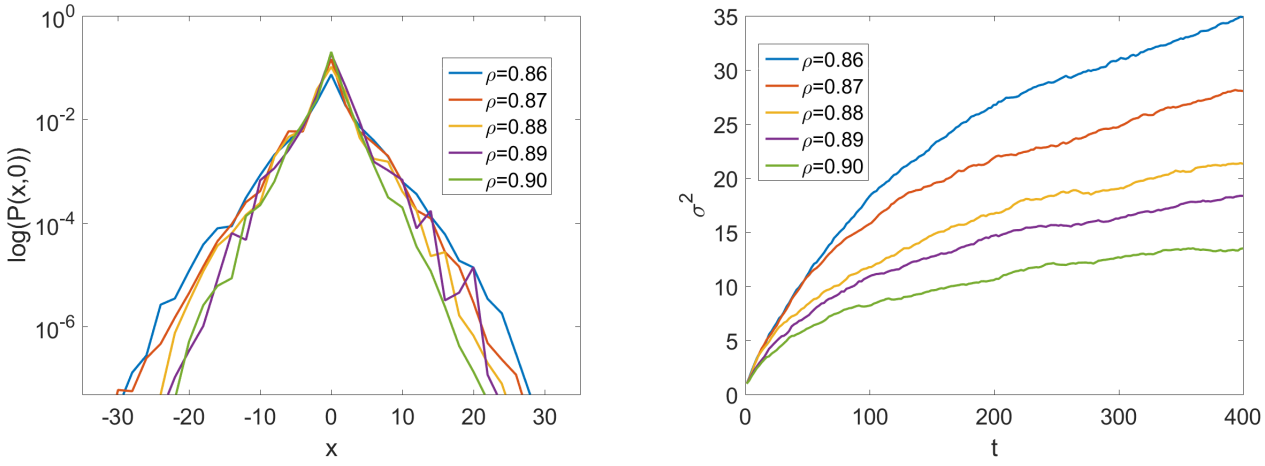

Figure 5.7: Cross-section of the probability distribution after 400 steps averaged over 10 iterations, semilogplot (on the left). The time-dependence of the corresponding variance σ^2 (on the right). The parameter of the coin operator set to $\rho = 0.86$,$\rho = 0.87$, $\rho = 0.88$, $\rho = 0.89$ and $\rho = 0.90$.

5.2 Elementary Manhattan cell with four different coins

Let us focus on the case of 4 different coin operators C_j acting in the elementary Manhattan cell. Firstly, we assume the coins to be real elements of SU(2), i.e.

$$C_j = \begin{pmatrix} \sqrt{1-\rho_j^2} & \rho_j^2 \\ -\rho_j^2 & \sqrt{1-\rho_j^2} \end{pmatrix}, \quad \rho_j \in [0,1], \quad j \in \{1,2,3,4\}. \tag{5.8}$$

The four-dimensional operator (3.8) then reads

$$C_M = \begin{pmatrix} \sqrt{1-\rho_1^2}\sqrt{1-\rho_2^2} & -\rho_1\sqrt{1-\rho_3^2} & \rho_2\sqrt{1-\rho_1^2} & \rho_1\rho_3 \\ \rho_1\sqrt{1-\rho_2^2} & \sqrt{1-\rho_1^2}\sqrt{1-\rho_3^2} & \rho_1\rho_2 & -\rho_3\sqrt{1-\rho_1^2} \\ -\rho_2\sqrt{1-\rho_4^2} & \rho_3\rho_4 & \sqrt{1-\rho_2^2}\sqrt{1-\rho_4^2} & \rho_4\sqrt{1-\rho_3^2} \\ \rho_2\rho_4 & \rho_3\sqrt{1-\rho_4^2} & -\rho_4\sqrt{1-\rho_2^2} & \sqrt{1-\rho_3^2}\sqrt{1-\rho_4^2} \end{pmatrix}. \tag{5.9}$$

Note that in this case the resulting probability distribution is no longer symmetric meaning that the choice of the cross-section can affect our conclusions. Therefore, we use the covariance matrix to find the directions in which the probability distribution spreads. The covariance matrix is symmetric and is given as

$$\Sigma = \begin{pmatrix} \sigma_x^2 & \mathrm{cov}(x,y) \\ \mathrm{cov}(y,x) & \sigma_y^2 \end{pmatrix}, \tag{5.10}$$

where σ_x^2, σ_y^2 is the variance computed along x axis, y axis, respectively. Covariance $\mathrm{cov}(x,y)$ is defined by

$$\mathrm{cov}(x,y) = \sum_{x,y\in\mathbb{Z}} (x-\mu(x))(y-\mu(y))P(x,y), \tag{5.11}$$

where $\mu(x)$, $\mu(y)$ are the mean values of the positions x and y. The eigenvectors of the covariance matrix then determines the main directions, in which the distribution spreads whereas the corresponding eigenvalues specify the shape of the distribution. That is, the spreading is greater in the direction of the eigenvector corresponding to the larger eigenvalue.

In the analysis of our results we utilize the information obtained from the covariance matrix and make the cross-sections in the directions given by its eigenvectors. However, we must also choose the cross-sections in accordance with the underlying discrete lattice.

According to the results obtained by Joye [20] the presence of localization is ensured in cases when C_M is close to a trapping permutation coin. Moreover, we know that the trapping effect for quantum walks on the Manhattan lattice is trivial. Consequently, these permutation matrices represent certain extreme cases of the trapping effect. Let us therefore begin the analysis with coin operators close to those exhibiting trapping. According to the results obtained for trapping, three of the coins C_j must be close to generalized reflections, i. e. without a loss of generality let us assume ρ_1, ρ_2, ρ_3 to be close to 1. The fourth parameter ρ_4 is an arbitrary number from [0,1]. In this case, there exists two trapping permutations

$$C_{\pi_1} = \begin{pmatrix} 0 & 0 & 0 & 1 \\ 0 & 0 & 1 & 0 \\ 0 & 1 & 0 & 0 \\ 1 & 0 & 0 & 0 \end{pmatrix}, \quad C_{\pi_2} = \begin{pmatrix} 0 & 0 & 0 & 1 \\ 0 & 0 & 1 & 0 \\ -1 & 0 & 0 & 0 \\ 0 & 1 & 0 & 0 \end{pmatrix}, \tag{5.12}$$

which are the extreme cases when $\rho_1 = \rho_2 = \rho_3 = \rho_4 = 1$ and $\rho_1 = \rho_2 = \rho_3 = 1, \rho_4 = 0$, respectively. Figure 5.2 depicts the dependence of the norm $\|C_M - C_{\pi_1}\|$ and $\|C_M - C_{\pi_2}\|$ on the parameter ρ_4 upon setting $\rho_1 = \rho_2 = \rho_3 = 0.999$. As a consequence, we expect localization at least for ρ_4 close to 0 and 1.

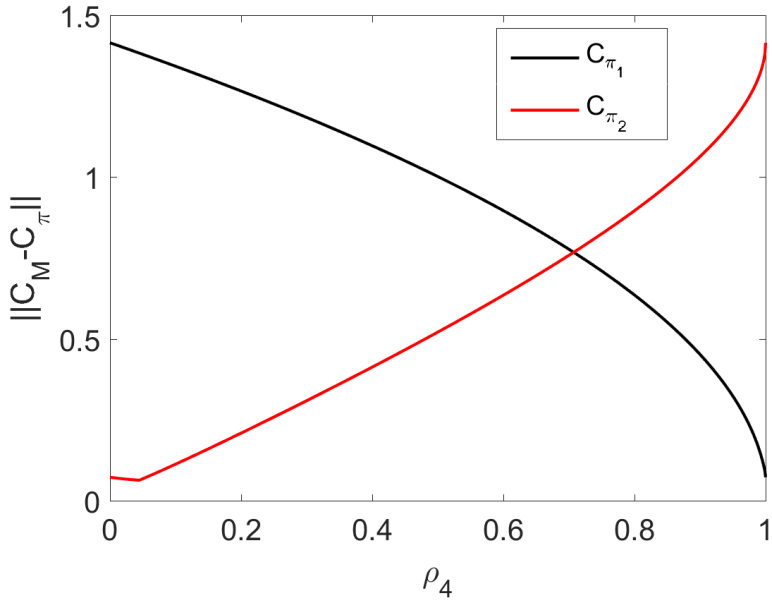

Figure 5.8: Dependence of the norm $\|C_M - C_{\pi_{1,1}}\|$ on the value of the parameter ρ_4 with $\rho_1 = \rho_2 = \rho_3 = 0.999$

5.2.1 Numerical simulations

In the numerical simulations we performed both 10000 iterations for 100 steps and 10 iterations for 400 steps. We set three parameters $\rho_1 = \rho_2 = \rho_3 = 0.999$ and varied the fourth parameter ρ_4 by 0.1 starting from $\rho_4 = 1.0$. Table 5.2.1 shows the eigenvectors and eigenvalues of the covariance matrix for both regimes of 10000 iterations–100 steps and 10 iterations–400 steps. We see that in both cases the axes of spreading can be well approximated by lines $x = y$ and $x = -y$ (see Figure (5.9). Moreover, except for $\rho_4 = 1.0$ the eigenvalues suggest that the probability distribution spreads more in the direction $x = -y$.
Let us first focus on the setting 10000 iterations–100 step. Figure 5.10 and Figure 5.11 depict the cross-sections of the averaged probability distribution along $x = y$ axis and $x = -y$ axis, respectively. In accordance with our expectations, the distribution spreads more in the direction $x = -y$ except for the case when $\rho_4 = 1.0$. The time dependence of the variance of the overall probability distribution is given by equation (5.4) and is depicted in Figure 5.12. Figure 5.12 suggests saturation of the discussed variance, however for certain values of the parameters, namely $\rho_4 = 0.4$, $\rho_4 = 0.6$, $\rho_4 = 0.7$ the results are inconclusive.
To obtain a better estimate of the asymptotic behaviour of the variance, we performed 10 iterations for quantum walk with 400 steps. As far as the shape of the cross-sections of the probability distribution is concerned (see Figure 5.13 and Figure 5.14), it is similar to the previous case of 100 steps. Moreover, the width of these cross-sections is comparable to that of Figure 5.10 and Figure 5.11, which also indicates that the propagation is suppressed. Finally, the time evolution of the variance plotted in Figure 5.15 appears to be bounded.
Based on the results obtained from numerical simulations presented in this section and section 5.1.1, we draw the following conclusion. The localization is present in the case when the real SU(2) coin operator C_M given by (5.9) is a small enough perturbation of the real SU(2) Manhattan trapping coin.

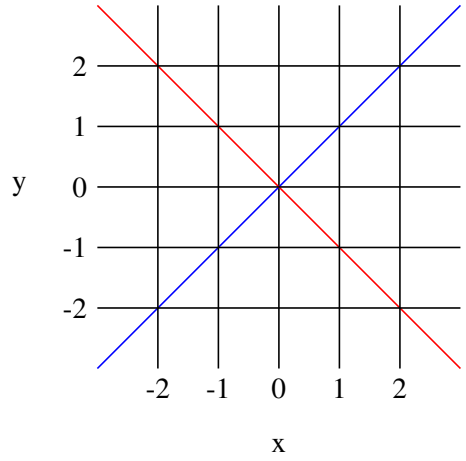

Figure 5.9: The cross-sections $x = -y$ (red) and $x = y$ (blue).

	100 steps				400 steps			
ρ_4	λ_1	λ_2	v_1	v_2	λ_1	λ_2	v_1	v_2
1.0	0.0137	0.0253	$\begin{pmatrix}-0.8879\\0.4600\end{pmatrix}$	$\begin{pmatrix}0.4600\\0.8879\end{pmatrix}$	0.0068	0.0579	$\begin{pmatrix}0.7064\\-0.7078\end{pmatrix}$	$\begin{pmatrix}-0.7078\\-0.7064\end{pmatrix}$
0.9	0.0583	0.2780	$\begin{pmatrix}-0.7259\\-0.6878\end{pmatrix}$	$\begin{pmatrix}-0.6878\\0.7259\end{pmatrix}$	0.1026	0.3839	$\begin{pmatrix}-0.7095\\-0.7047\end{pmatrix}$	$\begin{pmatrix}-0.7047\\0.7095\end{pmatrix}$
0.8	0.0759	0.4569	$\begin{pmatrix}-0.7394\\-0.6733\end{pmatrix}$	$\begin{pmatrix}-0.6733\\0.7394\end{pmatrix}$	0.0428	0.3140	$\begin{pmatrix}-0.7028\\-0.7113\end{pmatrix}$	$\begin{pmatrix}-0.7113\\0.7028\end{pmatrix}$
0.7	0.1544	0.5168	$\begin{pmatrix}-0.7171\\-0.6970\end{pmatrix}$	$\begin{pmatrix}-0.6970\\0.7171\end{pmatrix}$	0.0847	0.5858	$\begin{pmatrix}-0.7551\\-0.6556\end{pmatrix}$	$\begin{pmatrix}-0.6556\\0.7551\end{pmatrix}$
0.6	0.1050	0.6056	$\begin{pmatrix}-0.7018\\-0.7124\end{pmatrix}$	$\begin{pmatrix}-0.7124\\0.7018\end{pmatrix}$	0.1011	0.4156	$\begin{pmatrix}-0.6994\\-0.7147\end{pmatrix}$	$\begin{pmatrix}-0.7147\\0.6994\end{pmatrix}$
0.5	0.0946	0.5978	$\begin{pmatrix}-0.6755\\-0.7374\end{pmatrix}$	$\begin{pmatrix}-0.7374\\0.6755\end{pmatrix}$	0.1124	0.6646	$\begin{pmatrix}-0.6706\\-0.7418\end{pmatrix}$	$\begin{pmatrix}-0.7418\\0.6706\end{pmatrix}$
0.4	0.1278	0.7750	$\begin{pmatrix}-0.7077\\-0.7065\end{pmatrix}$	$\begin{pmatrix}-0.7065\\0.7077\end{pmatrix}$	0.1975	0.7225	$\begin{pmatrix}-0.7431\\-0.6692\end{pmatrix}$	$\begin{pmatrix}-0.6692\\0.7431\end{pmatrix}$
0.3	0.1290	0.6891	$\begin{pmatrix}-0.6977\\-0.7163\end{pmatrix}$	$\begin{pmatrix}-0.7163\\0.6977\end{pmatrix}$	0.0704	0.6351	$\begin{pmatrix}-0.7097\\-0.7046\end{pmatrix}$	$\begin{pmatrix}-0.7046\\0.7097\end{pmatrix}$
0.2	0.2042	0.6270	$\begin{pmatrix}-0.7927\\-0.6096\end{pmatrix}$	$\begin{pmatrix}-0.6096\\0.7927\end{pmatrix}$	0.0712	0.5726	$\begin{pmatrix}-0.6815\\-0.7318\end{pmatrix}$	$\begin{pmatrix}-0.7318\\0.6815\end{pmatrix}$
0.1	0.1808	0.8082	$\begin{pmatrix}-0.6921\\-0.7218\end{pmatrix}$	$\begin{pmatrix}-0.7218\\0.6921\end{pmatrix}$	0.1627	0.7523	$\begin{pmatrix}-0.6546\\-0.7560\end{pmatrix}$	$\begin{pmatrix}-0.7560\\0.6546\end{pmatrix}$
0.0	0.1864	0.2993	$\begin{pmatrix}-0.7506\\-0.6608\end{pmatrix}$	$\begin{pmatrix}-0.6608\\0.7506\end{pmatrix}$	0.0949	0.3780	$\begin{pmatrix}-0.7698\\-0.6383\end{pmatrix}$	$\begin{pmatrix}-0.6383\\0.7698\end{pmatrix}$

Table 5.1: Eigenvalues $\lambda_{1,2}$ and the corresponding eigenvectors $v_{1,2}$ of the covariance matrix for the averaged probability distribution for disordered quantum walks for 100 steps and 400 steps. The parameters of the coin operator (5.9) are given as $\rho_1 = \rho_2 = \rho_3 = 0.999$ and the ρ_4 is varied by 0.1.

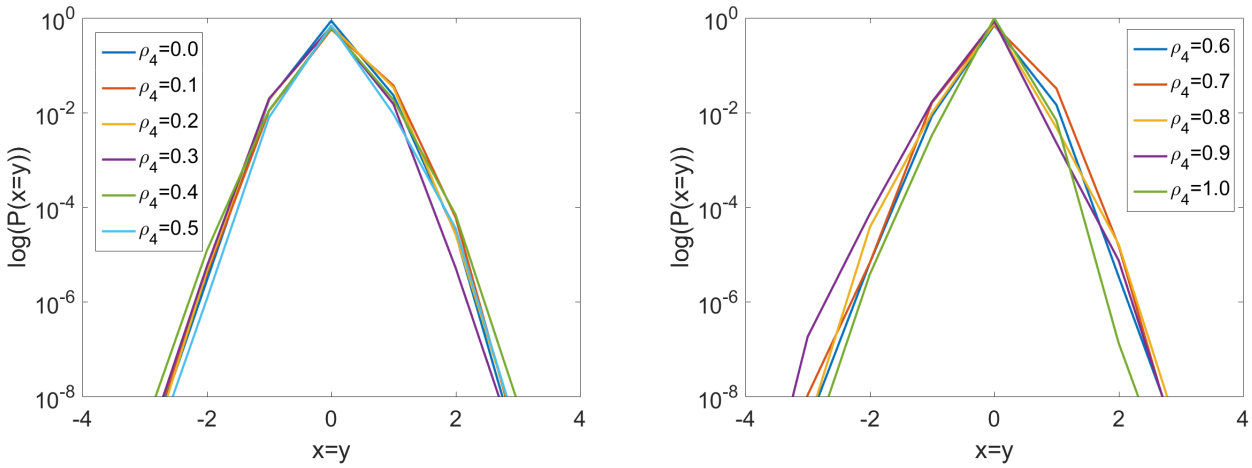

Figure 5.10: Cross-section along $x = y$ of the probability distribution after 100 steps averaged over 10000 iterations, semilogplot with the parameters $\rho_1 = \rho_2 = \rho_3 = 0.999$. On the left the parameter of the coin operator is set to $\rho_4 = 0.0$, $\rho_4 = 0.1$, $\rho_4 = 0.2$, $\rho_4 = 0.3$, $\rho_4 = 0.4$ and $\rho_4 = 0.5$. On the right the parameter of the coin operator is set to $\rho_4 = 0.6$, $\rho_4 = 0.7$, $\rho_4 = 0.8$, $\rho_4 = 0.9$ and $\rho_4 = 1.0$.

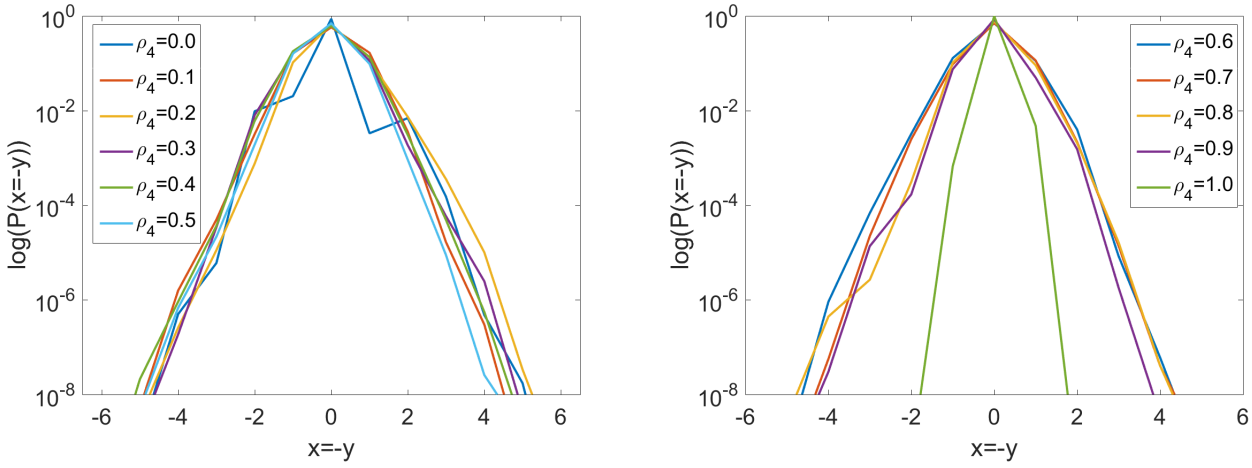

Figure 5.11: Cross-section along $x = -y$ of the probability distribution after 100 steps averaged over 10000 iterations, semilogplot with the parameters $\rho_1 = \rho_2 = \rho_3 = 0.999$. On the left the parameter of the coin operator is set to $\rho_4 = 0.0$, $\rho_4 = 0.1$, $\rho_4 = 0.2$, $\rho_4 = 0.3$, $\rho_4 = 0.4$ and $\rho_4 = 0.5$. On the right the parameter of the coin operator is set to $\rho_4 = 0.6$, $\rho_4 = 0.7$, $\rho_4 = 0.8$, $\rho_4 = 0.9$ and $\rho_4 = 1.0$.

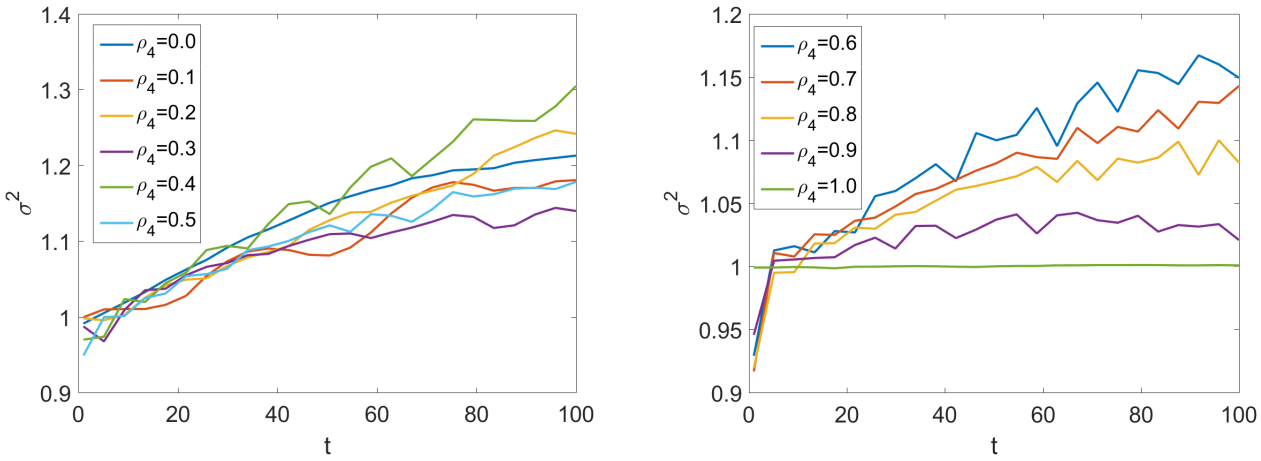

Figure 5.12: The time evolution of the variance of the probability distribution with the parameters $\rho_1 = \rho_2 = \rho_3 = 0.999$ averaged over 10000 iterations for 100 steps. On the left the parameter of the coin operator is set to $\rho_4 = 0.0$, $\rho_4 = 0.1$, $\rho_4 = 0.2$, $\rho_4 = 0.3$, $\rho_4 = 0.4$ and $\rho_4 = 0.5$. On the right the parameter of the coin operator is set to $\rho_4 = 0.6$, $\rho_4 = 0.7$, $\rho_4 = 0.8$, $\rho_4 = 0.9$ and $\rho_4 = 1.0$.

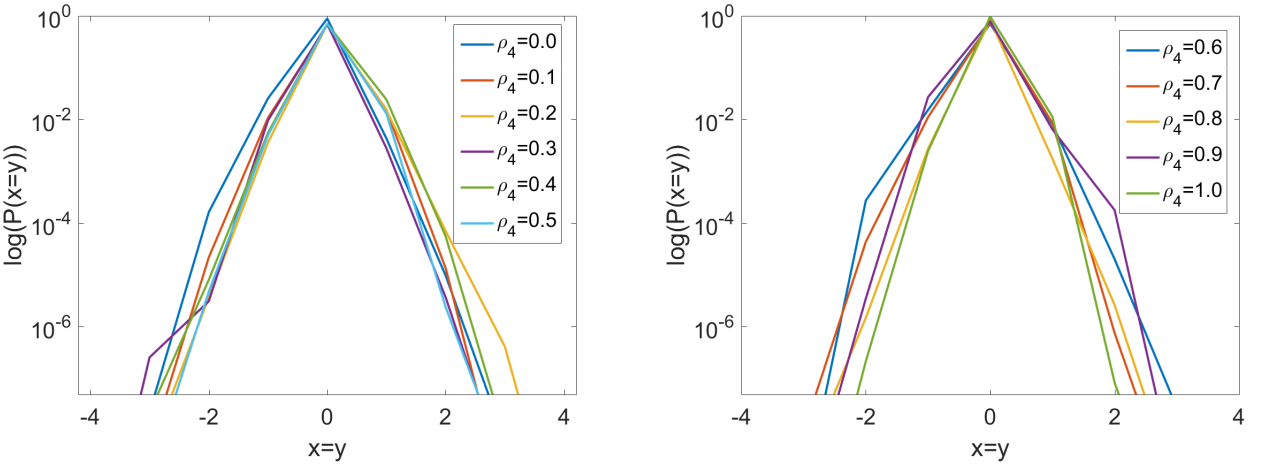

Figure 5.13: Cross-section along $x = y$ of the probability distribution after 400 steps averaged over 10 iterations, semilogplot with the parameters $\rho_1 = \rho_2 = \rho_3 = 0.999$. On the left the parameter of the coin operator is set to $\rho_4 = 0.0$, $\rho_4 = 0.1$, $\rho_4 = 0.2$, $\rho_4 = 0.3$, $\rho_4 = 0.4$ and $\rho_4 = 0.5$. On the right the parameter of the coin operator is set to $\rho_4 = 0.6$, $\rho_4 = 0.7$, $\rho_4 = 0.8$, $\rho_4 = 0.9$ and $\rho_4 = 1.0$.

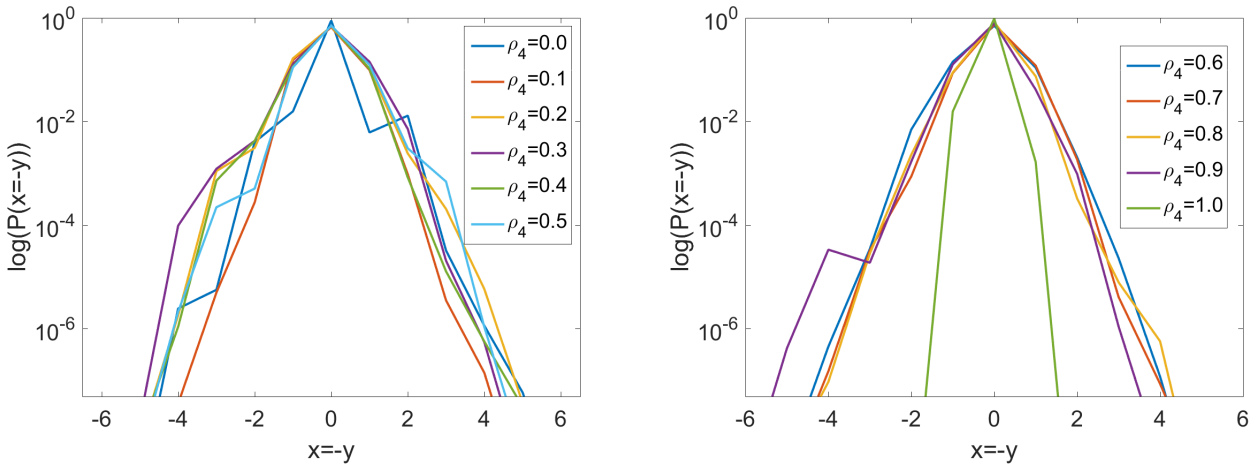

Figure 5.14: Cross-section along $x = -y$ of the probability distribution after 400 steps averaged over 10 iterations, semilogplot with the parameters $\rho_1 = \rho_2 = \rho_3 = 0.999$. On the left the parameter of the coin operator is set to $\rho_4 = 0.0$, $\rho_4 = 0.1$, $\rho_4 = 0.2$, $\rho_4 = 0.3$, $\rho_4 = 0.4$ and $\rho_4 = 0.5$. On the right the parameter of the coin operator is set to $\rho_4 = 0.6$, $\rho_4 = 0.7$, $\rho_4 = 0.8$, $\rho_4 = 0.9$ and $\rho_4 = 1.0$.

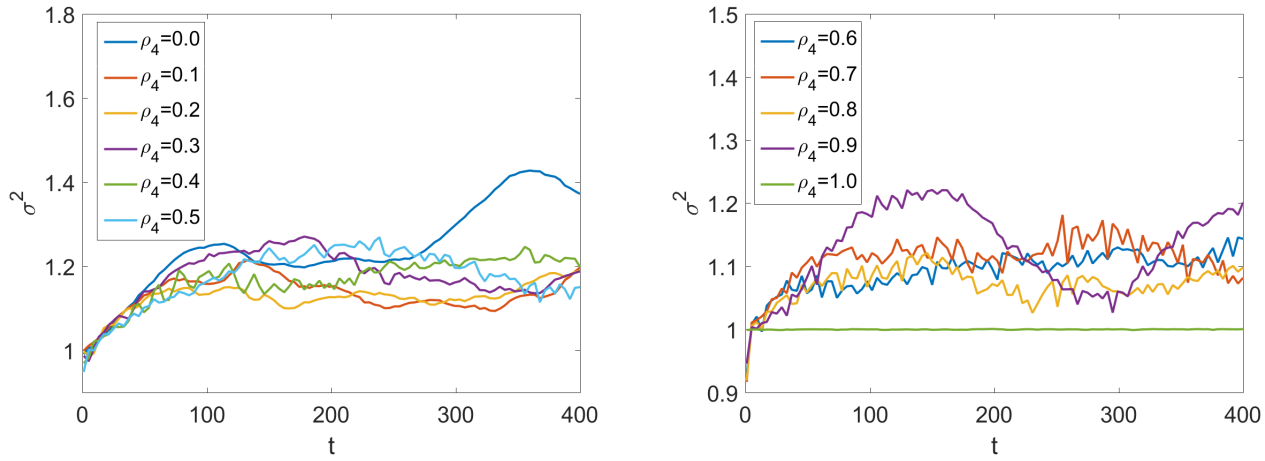

Figure 5.15: The time evolution of the variance of the probability distribution with the parameters $\rho_1 = \rho_2 = \rho_3 = 0.999$ averaged over 10 iterations for 400 steps. On the left the parameter of the coin operator is set to $\rho_4 = 0.0$, $\rho_4 = 0.1$, $\rho_4 = 0.2$, $\rho_4 = 0.3$, $\rho_4 = 0.4$ and $\rho_4 = 0.5$. On the right the parameter of the coin operator is set to $\rho_4 = 0.6$, $\rho_4 = 0.7$, $\rho_4 = 0.8$, $\rho_4 = 0.9$ and $\rho_4 = 1.0$..

5.2.2 Random coins

To estimate the behaviour of quantum walks with random phases in the case of four identical coin operators we varied the parameter ρ. However, in the case of 4 different coin operators in the Manhattan cell, the resulting four-dimensional coin operator (5.9) depends on 4 parameters. In the previous section we restricted ourselves to one special case when the coin represents a small perturbation of the trapping coin. To be able to estimate the behaviour when this condition does not hold, we choose the parameters ρ_1, ρ_2, ρ_3 and ρ_4 randomly from the interval [0,1].
We performed 100 quantum walks for different random choices of the coin to obtain preliminary results. For each of the choices we did 500 iterations for 100 steps. To be able to cover and analyse large enough sample, we focus only on two characteristics of the probability distribution. The first one is the minimum of norm $\|C_M - C_{\pi_i}\|$ where C_{π_i}, $i \in \{1, \cdots, 7\}$ is one of the 7 possible trapping permutations

$$C_{\pi_1} = \begin{pmatrix} 0 & 0 & 0 & 1 \\ 0 & 0 & 1 & 0 \\ 0 & 1 & 0 & 0 \\ 1 & 0 & 0 & 0 \end{pmatrix}, \quad C_{\pi_2} = \begin{pmatrix} 0 & 0 & 0 & 1 \\ 0 & 0 & 1 & 0 \\ -1 & 0 & 0 & 0 \\ 0 & 1 & 0 & 0 \end{pmatrix}, \quad C_{\pi_3} = \begin{pmatrix} 0 & -1 & 0 & 0 \\ 0 & 0 & 1 & 0 \\ 0 & 1 & 0 & 1 \\ 1 & 0 & 0 & 0 \end{pmatrix}, \quad C_{\pi_4} = \begin{pmatrix} 0 & -1 & 0 & 0 \\ 0 & 0 & 0 & -1 \\ -1 & 0 & 0 & 0 \\ 0 & 0 & -1 & 0 \end{pmatrix}$$

$$C_{\pi_5} = \begin{pmatrix} 0 & 0 & 1 & 0 \\ 1 & 0 & 0 & 0 \\ 0 & 0 & 0 & 1 \\ 0 & 1 & 0 & 0 \end{pmatrix}, \quad C_{\pi_6} = \begin{pmatrix} 0 & 0 & 1 & 0 \\ 0 & 0 & 0 & -1 \\ 0 & 1 & 0 & 0 \\ 1 & 0 & 0 & 0 \end{pmatrix}, \quad C_{\pi_7} = \begin{pmatrix} 0 & 0 & 0 & 1 \\ 1 & 0 & 1 & 0 \\ 0 & 1 & 0 & 0 \\ 0 & 0 & -1 & 0 \end{pmatrix}. \tag{5.13}$$

The second one is the value of the fit parameter a. To estimate the rate of spreading, we fitted the function $y(t) = b\, t^a$ to the variance $\sigma^2(t)$ of the overall probability distribution.
Figure 5.16 then depicts the dependence of the fit parameter a on the minimum of the norms. We see that for the majority of the quantum walks with the minimum of the norms in the interval [0.8, 1.5] the spreading is close to diffusion, since the variance behaves as $\sigma^2 \sim t$. On the other hand, with the norm increasing, ballistic propagation starts to prevail.
These numerical results lead us to the hypothesis that the Anderson localization on the Manhattan lattice with the disorder stemming from random phases arises only for the coin operator that represents a small perturbation of the coin operator that leads to the trapping effect.

5.3 Localization in quantum walks on the L-lattice

Unlike in case of quantum walks on the Manhattan lattice, localization of quantum walk on the L-lattice has already been studied numerically in [25] in context of two-dimensional split-step quantum walks.
Using numerical results, the authors of [25] argued that spatial disorder introduced via random phases leads to localization for an arbitrary two-dimensional split-step quantum walks except for coins that match the topological phase transition point. The phase transition is given by two lines $\theta_1 = \theta_2$ and $\theta_1 = -\theta_2$ (see Figure 5.17).
In [25] they took into consideration two split-step quantum walks with parameters $\theta_1 = 0.35\pi$, $\theta_2 = 0.15\pi$ (blue star Figure 5.17) and $\theta_1 = \pi/4$, $\theta_2 = -\pi/4$ (purple star Figure 5.17). Notice that the second choice of parameters is closely related to the quantum walk with the Hadamard coin

$$U_H = S_{DU}\, R(-\pi/4)\, S_{LR}^{-1}\, R(\pi/4). \tag{5.14}$$

In numerical simulations, the authors focused on two types of disorder stemming from random phases, namely the spin-independent disorder, in which case the multiplication of random phases acts as

$$D_\omega = \mathrm{diag}\left(\mathrm{e}^{\mathrm{i}\omega(x,y)}, \mathrm{e}^{\mathrm{i}\omega(x,y)}\right) \tag{5.15}$$

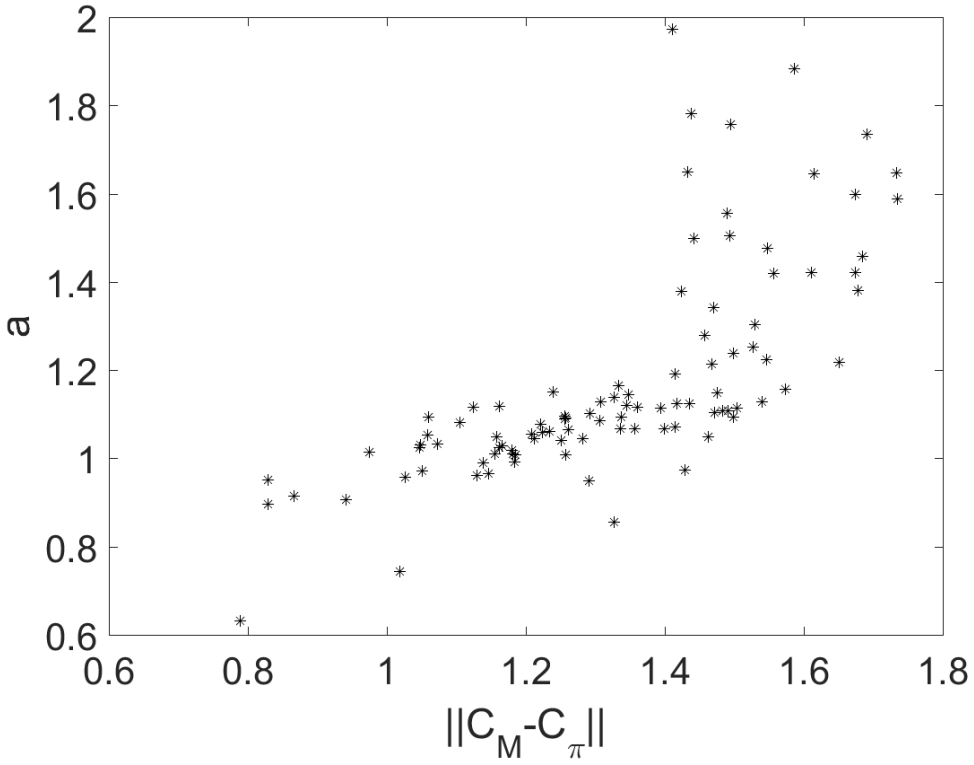

Figure 5.16: Dependence of the fit parameter a on the minimum of norms over all possible trapping permutations.

and the spin-dependent disorder, for which there is a phase shift by π in one of the diagonal elements

$$D_\omega = \mathrm{diag}\left(\mathrm{e}^{\mathrm{i}\omega(x,y)}, \mathrm{e}^{-\mathrm{i}\omega(x,y)}\right). \tag{5.16}$$

Figure 5.18 suggests the presence of localization in the case of the rotation coin with $\theta_1 = 0.35\pi$, $\theta_2 = 0.15\pi$ for both spin-dependent/independent disorder. On the other hand, parabolic shape of the cross-section for the disordered Hadamard walk is attributed to diffusive propagation. Let us note that in [25] the authors considered also disorder in the angle parameter. Contrary to expectations, this type of disorder led to diffusive propagation instead to localized quantum walks.

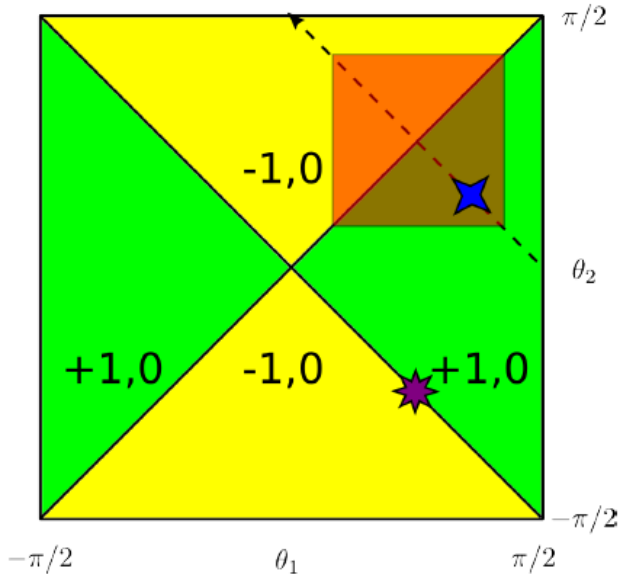

Figure 5.17: Phase diagram for the topological quantum numbers for two-dimensional split-step quantum walk. The blue star corresponds to the parameters $\theta_1 = 0.35\pi$, $\theta_2 = 0.15\pi$, the purple star represents the Hadamard walk (adopted from [25]).

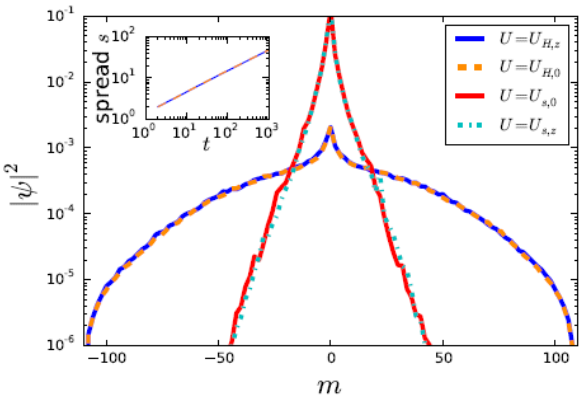

Figure 5.18: The cross-section of the probability distribution for split-step quantum walk after 1000 steps and 500 realizations. The blue and orange lines correspond to the Hadamard walk with spin-dependent/independent disorder, whereas red and green lines represent split-step walk with $\theta_1 = 0.35\pi$, $\theta_2 = 0.15\pi$ (adopted from [25]).

Conclusion

In this thesis we focused on the effect of localization in quantum walks on two specific cases of directed two-dimensional lattices, namely the Manhattan lattice and the L-lattice. We investigated both the effect of trapping that arises in the case of homogeneous quantum walks and on the Anderson localization which is related to the presence of static disorder.

In certain aspect, quantum walks on the Manhattan and the L-lattice lie between the two-state quantum walk on a line and the four-state quantum walk on an undirected two-dimensional lattice. On one hand, both Manhattan and the L-lattice are two-dimensional graphs. However, the lattices have directed edges, and on every vertex there are two incoming and two outgoing edges. Hence, for quantum walks on the Manhattan and the L-lattice the coin operators on the individual vertices are given by two-dimensional matrices, as in the case of the two-state quantum walk on a line. It was an open question whether localization in quantum walks on Manhattan and L-lattice will behave in a similar way to that for the two-state walk on a line or a four-state walk on a two-dimensional lattice.

In our analysis we have first showed that homogeneous quantum walks on the Manhattan lattice can be described using quantum walks on an undirected square lattice driven by four-dimensional coin operator of a specific form. For homogeneous quantum walks on the L-lattice this procedure can be taken further and one can show that they can be described using only two-dimensional coin operators. In fact, we showed that they are equivalent to the so-called two-dimensional split-step quantum walks or two-dimensional alternate quantum walks that have been studied previously.

The reduction of quantum walks on Manhattan and L-lattice to quantum walks on undirected lattices allowed us to investigate the trapping effect in detail. We determined the general form of a coin that leads to trapping. In both cases we found that trapping occurs only in trivial cases when the evolution operator possesses purely point spectrum. Due to the lack of the continuous spectrum the resulting trapping quantum walks on the Manhattan lattice, as well as on the L-lattice, do not propagate. Hence, the trappping effect on these two oriented lattices is similar to that for the two-state quantum walk on a line. This result can be anticipated for the L-lattice, since the quantum walk is described by two-dimensional coin operator. On the other hand, the walk on the Manhattan lattice can be described using four-dimensional coin operators which in principle allow for non-trivial trapping effect. However, the form of the coin operator proved to be too restricting.

In the last chapter we dealt mainly with Anderson localization on the Manhattan lattice. We restricted ourselves only to static disorder introduced via independent, identically distributed random phases. Motivated by known analytical results, we performed numerical simulations. Based on these numerical data we estimated the asymptotic behaviour from two characteristics of our interest: the cross-section of the averaged probability distribution and the time-dependence of the variance of the overall probability distribution. The numerical simulations performed for the elementary Manhattan cell with four identical coins suggest presence of localization only in the case when the four-dimensional coin operator is close to anti-diagonal matrix. In the case of four different coin operators within the elementary Manhattan cell localization appears to be present for coins that represent a small perturbation from those exhibiting

trapping effect. These results led us to the hypothesis that localization in quantum walks on the Manhattan lattice arises only for coins close to the trapping coins. We note that for the L-lattice the situation is different. Indeed, the study of Anderson localization in [23] proved that it arises for almost arbitrary choice of the coin operator, as in the case of one-dimensional quantum walks.

Many interesting questions remain open. To our best knowledge, except for Joye's results [20], Anderson localization has not been proved analytically in dimensions higher than one. Moreover, these results only deal with coins in a specific form. The question then arises, whether this effect can be observed for a broader range of four-dimensional coin operators on a square lattices or not. This question has been partially answered in this thesis where we considered one special case of the underlying lattice – the Manhattan lattice.

Appendix A

A.1 Trapping effect in quantum walks on the Manhattan lattice

In the following we focus on the details of the calculations outlined in section 3.2. Since the characteristic equation (3.14) holds for arbitrary k, l we obtain following relations for the coin parameters a_i, b_i, c_i, d_i, $i \in \{1,2,3,4\}$

$$\begin{aligned}
\mathrm{e}^{-\mathrm{i}l}: &\quad -a_1d_3\mathrm{e}^{3\mathrm{i}\varphi} - a_2b_1b_3c_1c_3d_4\mathrm{e}^{\mathrm{i}\varphi} + a_1a_2b_3c_3d_1d_4\mathrm{e}^{\mathrm{i}\varphi} + a_2a_3b_1c_1d_3d_4\mathrm{e}^{\mathrm{i}\varphi} - a_1a_2a_3d_1d_3d_4\mathrm{e}^{\mathrm{i}\varphi} = 0\\
\mathrm{e}^{\mathrm{i}l}: &\quad -a_4d_2\mathrm{e}^{3\mathrm{i}\varphi} - a_3b_2b_4c_2c_4d_1\mathrm{e}^{\mathrm{i}\varphi} + a_2a_3b_4c_4d_1d_2\mathrm{e}^{\mathrm{i}\varphi} + a_3a_4b_2c_2d_1d_4\mathrm{e}^{\mathrm{i}\varphi} - a_2a_3a_4d_1d_2d_4\mathrm{e}^{\mathrm{i}\varphi} = 0\\
\mathrm{e}^{\mathrm{i}k}: &\quad -a_3d_4\mathrm{e}^{3\mathrm{i}\varphi} - a_1a_3a_4d_2d_3d_4\mathrm{e}^{\mathrm{i}\varphi} + a_1a_4b_3c_3d_2d_4\mathrm{e}^{\mathrm{i}\varphi} + a_1a_3b_4c_4d_2d_3\mathrm{e}^{\mathrm{i}\varphi} - a_1b_3b_4c_3c_4d_2\mathrm{e}^{\mathrm{i}\varphi} = 0\\
\mathrm{e}^{-\mathrm{i}k}: &\quad -a_2d_1\mathrm{e}^{3\mathrm{i}\varphi} - a_4b_1b_2c_1c_2d_3\mathrm{e}^{\mathrm{i}\varphi} + a_1a_4b_2c_2d_1d_3\mathrm{e}^{\mathrm{i}\varphi} + a_2a_4b_1c_1d_2d_3\mathrm{e}^{\mathrm{i}\varphi} - a_1a_2a_4d_1d_2d_3\mathrm{e}^{\mathrm{i}\varphi} = 0
\end{aligned} \tag{A.1}$$

$$\begin{aligned}
\mathrm{e}^{\mathrm{i}(k-l)}: &\quad a_1a_3d_3d_4\mathrm{e}^{2\mathrm{i}\varphi} - a_1b_3c_3d_4\mathrm{e}^{2\mathrm{i}\varphi} = 0\\
\mathrm{e}^{\mathrm{i}(k+l)}: &\quad a_3a_4d_2d_4\mathrm{e}^{4\mathrm{i}\varphi} - a_3b_4c_4d_2\mathrm{e}^{4\mathrm{i}\varphi} = 0\\
\mathrm{e}^{\mathrm{i}(-k-l)}: &\quad a_1a_2d_1d_3\mathrm{e}^{4\mathrm{i}\varphi} - a_2b_1c_1d_3\mathrm{e}^{4\mathrm{i}\varphi} = 0\\
\mathrm{e}^{\mathrm{i}(-k+l)}: &\quad a_2a_4d_1d_2\mathrm{e}^{4\mathrm{i}\varphi} - a_4b_2c_2d_1\mathrm{e}^{4\mathrm{i}\varphi} = 0
\end{aligned} \tag{A.2}$$

$$\mathrm{e}^{4\mathrm{i}\varphi} - b_1b_2b_3b_4\mathrm{e}^{2\mathrm{i}\varphi} + a_1a_4d_2d_3\mathrm{e}^{2\mathrm{i}\varphi} + a_2a_3d_1d_4\mathrm{e}^{2\mathrm{i}\varphi} - c_1c_2c_3c_4\mathrm{e}^{2\mathrm{i}\varphi} + \det C = 0 \tag{A.3}$$

where

$$\begin{aligned}
\det C = {} & a_1a_2a_3a_4d_1d_2d_3d_4 - a_1a_2a_3b_4c_4d_1d_2d_3 - a_1a_2a_4b_3c_3d_1d_2d_4 + a_1a_2b_3b_4c_3c_4d_1d_2\\
& - a_1a_3a_4b_2c_2d_1d_3d_4 + a_1a_3b_2b_4c_2c_4d_1d_3 + a_1a_4b_2b_3c_2c_3d_1d_4 - a_1b_2b_3b_4c_2c_3c_4d_1\\
& - a_2a_3a_4b_1c_1d_2d_3d_4 + a_2a_3b_1b_4c_1c_4d_2d_3 + a_2a_4b_1b_3c_1c_3d_2d_4 - a_2b_1b_3b_4c_1c_3c_4d_2\\
& + a_3a_4b_1b_2c_1c_2d_3d_4 - a_3b_1b_2b_4c_1c_2c_4d_3 - a_4b_1b_2b_3c_1c_2c_3d_4 + b_1b_2b_3b_4c_1c_2c_3c_4.
\end{aligned} \tag{A.4}$$

Relations (A.2) imply

$$a_1d_4 = 0 \quad a_2d_3 = 0 \quad a_3d_2 = 0 \quad a_4d_1 = 0 \tag{A.5}$$

since the determinant of the unitary matrices (3.3) is never equal to zero. There exist 16 possible combinations how these conditions can be satisfied. If we also take into account the conditions on the unitarity of matrices (3.3), four of these combinations gives trivial solution in the form of antidiagonal two-dimensional matrices whereas eight of these combinations immediately yield solution in the form of

$$C_i = \begin{pmatrix} 0 & c_i \\ b_i & 0 \end{pmatrix}, \quad C_j = \begin{pmatrix} 0 & c_j \\ b_j & 0 \end{pmatrix}, \quad C_k = \begin{pmatrix} 0 & c_k \\ b_k & 0 \end{pmatrix}, \quad C_l = \begin{pmatrix} a_l & c_l \\ b_l & d_l \end{pmatrix}, \tag{A.6}$$

where i, j, k, l are pair-wise distinct indexes from $\{1, 2, 3, 4\}$. It can be readily verified that the equations (A.1) also imply solution in the form of (A.6) for the last four of the 16 combinations. The equation (A.3) then puts another restriction on the matrices (A.6) in the form of

$$\mathrm{e}^{4\mathrm{i}\varphi} - b_i b_j b_k b_l \mathrm{e}^{2\mathrm{i}\varphi} - c_i c_j c_k c_l \mathrm{e}^{2\mathrm{i}\varphi} - b_i b_j b_k c_i c_j c_k (a_l d_l - b_l c_l) = 0. \tag{A.7}$$

A.2 Trapping effect in quantum walks on the L-lattice

Let us now turn to the details of the calculations touched upon in 4.2. The characteristic equation (4.12) can be readily separated in the following manner, as it holds for arbitrary $k, l \in [-\pi, \pi]$

$$\mathrm{e}^0 : \mathrm{e}^{2\mathrm{i}\varphi} - a_1 b_2 c_4 d_3 \mathrm{e}^{\mathrm{i}\varphi} - a_2 b_3 c_1 d_4 \mathrm{e}^{\mathrm{i}\varphi} - a_3 b_4 c_2 d_1 \mathrm{e}^{\mathrm{i}\varphi} - a_4 b_1 c_3 d_2 \mathrm{e}^{\mathrm{i}\varphi} + \det C = 0 \tag{A.8}$$

$$\begin{aligned}
\mathrm{e}^{-2\mathrm{i}k} &: -a_1 a_4 b_2 c_3 \mathrm{e}^{\mathrm{i}\varphi} - a_2 a_3 b_4 c_1 \mathrm{e}^{\mathrm{i}\varphi} = 0 \\
\mathrm{e}^{-2\mathrm{i}l} &: -a_1 a_2 b_3 c_4 \mathrm{e}^{\mathrm{i}\varphi} - a_3 a_4 b_1 c_2 \mathrm{e}^{\mathrm{i}\varphi} = 0 \\
\mathrm{e}^{2\mathrm{i}k} &: -b_1 c_4 d_2 d_3 \mathrm{e}^{\mathrm{i}\varphi} - b_3 c_2 d_1 d_4 \mathrm{e}^{\mathrm{i}\varphi} = 0 \\
\mathrm{e}^{2\mathrm{i}l} &: -b_2 c_1 d_3 d_4 \mathrm{e}^{\mathrm{i}\varphi} - b_4 c_3 d_1 d_2 \mathrm{e}^{\mathrm{i}\varphi} = 0 \\
\mathrm{e}^{-2\mathrm{i}(k+l)} &: -a_1 a_2 a_3 a_4 \mathrm{e}^{\mathrm{i}\varphi} = 0 \\
\mathrm{e}^{2\mathrm{i}(k-l)} &: -b_1 b_3 c_2 c_4 \mathrm{e}^{\mathrm{i}\varphi} = 0 \\
\mathrm{e}^{2\mathrm{i}(-k+l)} &: -b_2 b_4 c_1 c_3 \mathrm{e}^{\mathrm{i}\varphi} = 0 \\
\mathrm{e}^{2\mathrm{i}(k+l)} &: -d_1 d_2 d_3 d_4 \mathrm{e}^{\mathrm{i}\varphi} = 0,
\end{aligned} \tag{A.9}$$

The relations (A.9) together with conditions on the unitarity of the coins $C_1,\ C_2,\ C_3,\ C_4$ immediately yield solution in the form of

$$C_i = \begin{pmatrix} 0 & \mathrm{e}^{\mathrm{i}\alpha_i} \\ \mathrm{e}^{\mathrm{i}\beta_i} & 0 \end{pmatrix}, \quad C_j = \begin{pmatrix} 0 & \mathrm{e}^{\mathrm{i}\alpha_j} \\ \mathrm{e}^{\mathrm{i}\beta_j} & 0 \end{pmatrix}, \quad C_k = \begin{pmatrix} \mathrm{e}^{\mathrm{i}\alpha_k} & 0 \\ 0 & \mathrm{e}^{\mathrm{i}\beta_k} \end{pmatrix}, \quad C_l = \begin{pmatrix} a_l & c_l \\ b_l & d_l \end{pmatrix} \tag{A.10}$$

or

$$C_i = \begin{pmatrix} \mathrm{e}^{\mathrm{i}\alpha_i} & 0 \\ 0 & \mathrm{e}^{\mathrm{i}\beta_i} \end{pmatrix}, \quad C_j = \begin{pmatrix} \mathrm{e}^{\mathrm{i}\alpha_j} & 0 \\ 0 & \mathrm{e}^{\mathrm{i}\beta_j} \end{pmatrix}, \quad C_k = \begin{pmatrix} 0 & \mathrm{e}^{\mathrm{i}\alpha_k} \\ \mathrm{e}^{\mathrm{i}\beta_k} & 0 \end{pmatrix}, \quad C_l = \begin{pmatrix} a_l & c_l \\ b_l & d_l \end{pmatrix} \tag{A.11}$$

where $i, j, k, l \in \{1, 2, 3, 4\}$ are pair-wise distinct indices satisfying $(i, j) = (1, 3)$ or $(i, j) = (2, 4)$. These solutions are further restricted by conditions imposed by equation (A.8).

Bibliography

[1] Y. Aharonov, L. Davidovich, and N. Zagury. Quantum random walks. *Physical Review A*, 48:1687, 1993.

[2] D. Meyer. From quantum cellular automata to quantum lattice gases. *Journal of Statistical Physics*, 85:551, 1996.

[3] A. Einstein. Über die von der molekularkinetischen theorie der wärme geforderte bewegung von in ruhenden flüssigkeiten suspendierten teilchen. *Annalen der Physik*, 7:549, 1905.

[4] N. Shenvi, J. Kempe, and K. B. Whaley. Quantum random-walk search algorithm. *Physical Review A*, 67:052307, 2003.

[5] K. Manouchehri and J. Wang. *Physical Implementation of Quantum Walks*. Springer Publishing Company, Berlin, 2014.

[6] P. W. Anderson. Absence of diffusion in certain random lattices. *Physical Review*, 109:1492, 1958.

[7] E. J. Beamond, A. L. Owczarek, and J. Cardy. Quantum and classical localisation and the Manhattan lattice. *Journal of Physics A*, 36:10251, 2003.

[8] E. J. Beamond, J. Cardy, and J.T. Chalker. Quantum and classical localisation, the spin quantum Hall effect and generalizations. *Physical Review B*, 65:214301, 2002.

[9] A. Ambainis, E. Bach, A. Nayak, A. Vishwanath, and J. Watrous. One-dimensional quantum walks. In *Proceedings of the Thirty-third Annual ACM Symposium on Theory of Computing*, STOC '01, pages 37–49, New York, NY, USA, 2001.

[10] A. Kempf and R. Portugal. Group velocity of discrete-time quantum walks. *Physical Review A*, 79(5):052317, 2009.

[11] N. Inui, N. Konno, and E. Segawa. One-dimensional three-state quantum walk. *Physical Review E*, 72:056112, 2005.

[12] M. Štefaňák, B. Kollár, T. Kiss, and I. Jex. Full revivals in 2D quantum walks. *Physica Scripta Volume T*, 140(1):014035, 2010.

[13] N. Inui, Y. Konishi, and N. Konno. Localization of two-dimensional quantum walks. *Physical Review A*, 69:052323, 2004.

[14] B. Kollár, T. Kiss, and I. Jex. Strongly trapped two-dimensional quantum walks. *Physical Review A*, 91(2):022308, 2015.

[15] K. Werner. An invitation to random Schrödinger operators. *arXiv:0709.3707*, 2007.

[16] A. Joye, E. Hamza, and G. Stolz. Dynamical localization for unitary Anderson models. *Mathematical Physics, Analysis and Geometry*, 12:381, 2009.

[17] P. D. Hislop. Lectures on random Schrödinger operators. *Contemporary Mathematics*, 476:41, 2008.

[18] A. Joye. Random unitary models and their localization properties. *Entropy and the Quantum II, Contemporary Mathematics*, 552:117, 2011.

[19] A. Klein. Multiscale analysis and localization of random operators. *arXiv:0708.2292*, 2007.

[20] A. Joye. Dynamical localization for d-dimensional random quantum walks. *Quantum Information Processing*, 11(5):1251, 2012.

[21] A. Joye and M. Merkli. Dynamical localization of quantum walks in random environments. *Journal of Statistical Physics*, 140(6):1025, 2010.

[22] A. Ahlbrecht, V.B. Scholz, and A.H. Werner. Disordered quantum walks in one lattice dimension. *Journal of Mathematical Physics*, 52:102201, 2011.

[23] A. Joye. Random time-dependent quantum walks. *Communications in Mathematical Physics*, 370:65, 2011.

[24] C. di Franco, M. Mc Gettrick, and T. Busch. Mimicking the probability distribution of a two-dimensional Grover walk with a single-qubit coin. *Physical Review Letters*, 106(8):080502, 2011.

[25] J. M. Edge and J. K. Asboth. Localization, delocalization, and topological transitions in disordered two-dimensional quantum walks. *Physical Review B*, 91:104202, 2015.